scientific reports

Check for updates

OPEN

Efficient DC motor speed control using a novel multi-stage FOPD(1 + PI) controller optimized by the Pelican optimization algorithm

Mostafa Jabari[1], Serdar Ekinci[2], Davut Izci[2,3,4], Mohit Bajaj[5,6,7]✉ & Ievgen Zaitsev[8,9]✉

This paper introduces a novel multi-stage FOPD(1 + PI) controller for DC motor speed control, optimized using the Pelican Optimization Algorithm (POA). Traditional PID controllers often fall short in handling the complex dynamics of DC motors, leading to suboptimal performance. Our proposed controller integrates fractional-order proportional-derivative (FOPD) and proportional-integral (PI) control actions, optimized via POA to achieve superior control performance. The effectiveness of the proposed controller is validated through rigorous simulations and experimental evaluations. Comparative analysis is conducted against conventional PID and fractional-order PID (FOPID) controllers, fine-tuned using metaheuristic algorithms such as atom search optimization (ASO), stochastic fractal search (SFS), grey wolf optimization (GWO), and sine-cosine algorithm (SCA). Quantitative results demonstrate that the FOPD(1 + PI) controller optimized by POA significantly enhances the dynamic response and stability of the DC motor. Key performance metrics show a reduction in rise time by 28%, settling time by 35%, and overshoot by 22%, while the steady-state error is minimized to 0.3%. The comparative analysis highlights the superior performance, faster response time, high accuracy, and robustness of the proposed controller in various operating conditions, consistently outperforming the PID and FOPID controllers optimized by other metaheuristic algorithms. In conclusion, the POA-optimized multi-stage FOPD(1 + PI) controller presents a significant advancement in DC motor speed control, offering a robust and efficient solution with substantial improvements in performance metrics. This innovative approach has the potential to enhance the efficiency and reliability of DC motor applications in industrial and automotive sectors.

Keywords DC motor control, Fractional-order controller, Metaheuristic algorithms, Pelican optimization Algorithm, Performance optimization, PID controller, Speed control, Stability improvement

List of symbols

DC	Direct current
POA	Pelican optimization algorithm
$ITAE$	Integral of time-weighted absolute error
PI	Proportional–integral
FLC	Fuzzy logic controller

[1]Faculty of Electrical Engineering, Sahand University of Technology, Tabriz, Iran. [2]Department of Computer Engineering, Batman University, Batman 72100, Turkey. [3]Applied Science Research Center, Applied Science Private University, Amman 11931, Jordan. [4]MEU Research Unit, Middle East University, Amman 11831, Jordan. [5]Department of Electrical Engineering, Graphic Era (Deemed to be University), Dehradun 248002, India. [6]Graphic Era Hill University, Dehradun 248002, India. [7] College of Engineering, University of Business and Technology, Jeddah 21448, Saudi Arabia. [8]Department of Theoretical Electrical Engineering and Diagnostics of Electrical Equipment, Institute of Electrodynamics, National Academy of Sciences of Ukraine, Beresteyskiy, 56, Kyiv-57 03680, Ukraine. [9]Center for Information-Analytical and Technical Support of Nuclear Power Facilities Monitoring, National Academy of Sciences of Ukraine, Akademika Palladina Avenue, 34-A, Kyiv, Ukraine. ✉email: thebestbajaj@gmail.com; zaitsev@i.ua

PID	Proportional–integral–derivative
$FOPID$	Fractional order PID
ASO	Atom search optimization
SFS	Stochastic fractal search
GWO	Gray wolf optimization
SCA	Sine–cosine algorithm
EMF	Back electromotive force
DE	Differential evolution
OBL	Opposition- based learning
LFD	Lévy flight distribution
ΔS	Speed error between reference and actual angular speeds
$ChASO$	Chaotic atom search optimization
SA	Simulated annealing
MLP	Multilayer perceptron
HGO	Henry gas solubility optimization
GOA	Gazelle optimization algorithm
GSO	Gazelle simplex optimizer
HHO	Harris Hawks optimization
$OBL/HGSO$	Opposition-based Henry gas solubility optimization
WOA	Whale optimization algorithm
$hASO-SA$	Hybrid atom search optimization with simulated annealing
$LFDNM$	Hybrid Lévy flight distribution and Nelder–Mead
$OBL-MRFO-SA$	Opposition-based hybrid manta ray foraging optimization and simulated annealing algorithm
PSO	Particle swarm optimization
K_P, K_{PP}	Proportional gains of multi-stage controller
K_D	Derivative gain of multi-stage controller
$e(t)$	Error signal between reference speed and actual speed
NNC	Neural network controller
e_a	Armature voltage
R_a	Armature resistance
L_a	Armature inductance
E_a	Input voltage
I_f	Field current
I_a	Armature current
e_b	Induced voltage
k_b	Electromotive force constant
ω_m	Angular speed of motor shaft
J	Inertia torque of motor
B	Motor friction constant
T	Motor torque
T_L	Motor load torque
K	Motor torque constant
CF	Cost function
IAE	Integral of absolute error
$ITSE$	Integral of time-weighted square error
ISE	Integral of square error
ω_{ref}	Speed reference motor
K_I	Integral gains of multi-stage controller
λ, μ	Integral and derivative order

The application of DC motors is of significant importance within the engineering domain, primarily attributed to their manageability, longevity, and cost-efficiency according to Deng, et al.[1] and Varatharajan, et al.[2]. Nevertheless, the management of speed poses a formidable challenge owing to intricate surroundings and nonlinear dynamics, resulting in potential instability[3,4]. Furthermore, DC motors exhibit high sensitivity towards disturbances in load, consequently leading to notable speed deviations. These disturbances may stem from alterations in load torque, fluctuations in power supply, or external environmental influences[2,5]. Moreover, fluctuations in motor characteristics such as variations in resistance, inductance, or back electromotive force (EMF) constant, attributed to factors like aging, temperature fluctuations, or inconsistencies in manufacturing, can introduce challenges in upholding consistent motor performance. This aspect becomes particularly critical in domains such as robotics, industrial automation, and electric vehicles, where even slight deviations in speed can trigger substantial performance issues or operational breakdowns[3,6,7].

Several control methodologies have been developed in order to tackle these obstacles. The PID controllers are frequently employed in industrial settings because of their straightforwardness and efficiency in improving the transient and steady-state behaviors of systems[8]. These controllers modulate the control input by monitoring the error signal, offering a well-rounded approach to error rectification. Nonetheless, conventional PID controllers may encounter difficulties in handling the nonlinear and variable characteristics of DC motor dynamics, particularly in the presence of significant disturbances or parameter variations[9]. To enhance performance, advanced control approaches have been explored, with FOPID controllers emerging as a viable solution[10].

FOPID controllers exhibit superior performance and resilience compared to the traditional PID controllers in scenarios involving complex systems like DC motors that manifest nonlinearities and uncertainties[11,12]. By incorporating fractional calculus, FOPID controllers extend the capabilities of conventional PID controllers, enabling more adaptable tuning of control actions[13]. This enhanced flexibility equips FOPID controllers to manage the intricacies of DC motor control more effectively, leading to improved robustness and stability[11,14].

In the realm of DC motor speed control, various control strategies beyond PID and FOPID controllers have been developed to enhance precision and robustness. Neural network controllers (NNCs), as discussed in[15], can effectively learn and adapt to the intricate dynamics of the motor system. Fuzzy logic controllers (FLCs), as highlighted in[16 and 17], utilize a rule-based approach to manage uncertainties and imprecise data, offering a flexible solution. Adaptive controllers, as mentioned in[18], dynamically adjust their parameters to accommodate evolving system dynamics, ensuring real-time optimization. Additionally, sliding mode controllers, as detailed in[19], maintain stability by employing high-frequency switching, providing a robust mechanism to counter disturbances and parameter variations in DC motor speed control systems.

To optimize controller parameters, various metaheuristic optimization algorithms are utilized, mimicking natural processes for efficient solutions in complex spaces. Particle swarm optimization (PSO) and differential evolution (DE) excel in exploring global optima[20]. GWO and enhanced version of SCA leverage wolf social behavior and mathematical functions, respectively, for successful parameter fine-tuning[21,22]. The hybrid SFS (HSFS) algorithm, combining SFS and pattern search optimization, has shown remarkable advancements in balancing exploration and exploitation phases for optimization tasks[23].

Hekimoğlu[11] presents a promising approach to optimally tune FOPID controllers for DC motor speed control using a novel chaotic optimization algorithm, addressing a significant challenge in the field of motor control and automation. The paper proposes the use of the chaotic atom search optimization (ChASO) algorithm to optimally tune the five parameters $(K_P, K_I, K_D, \lambda, \mu)$ of the FOPID controller for a DC motor speed control system. Eker, et al.[24] utilizes a novel hybrid optimization algorithm that combines the ASO algorithm with the simulated annealing (SA) algorithm. This hybrid algorithm is applied to two challenging optimization problems: training a multilayer perceptron (MLP) neural network and tuning a controller for DC motor speed control.

Ekinci, et al.[25] presents a promising approach to optimally tune PID controllers for DC motor speed control using a novel physics-inspired optimization algorithm, the opposition-based Henry gas solubility optimization (OBL/HGSO), addressing a significant challenge in the field of motor control and automation. The proposed OBL/HGSO algorithm combines the HGSO algorithm with the OBL strategy, which aims to improve the exploration and exploitation capabilities of the optimization process. In Idir, et al.[26] presents a novel approach for enhancing the performance of DC motor speed control systems. The study leverages the henry gas solubility optimization (HGSO) algorithm to fine-tune a fractionalized PID controller, resulting in improved precision and efficiency. Ekinci, et al.[27] presents a novel hybrid optimization algorithm (OBL-MRFO-SA) for optimally tuning a FOPID controller for precise speed control of DC motors, addressing the challenges posed by nonlinearities and complex optimization problems. Izci[28] by using a novel hybrid optimization algorithm combining the Lévy flight distribution and the Nelder–Mead simplex method for optimally tuning a PID controller to achieve precise speed regulation of DC motors, addressing a significant challenge in the field of motor control and automation. Ekinci, et al.[29] present a new method called the gazelle simplex optimizer (GSO), aimed at improving PID controllers to precisely control the speed of DC motors. Results demonstrate the superior performance of the GSO-PID controller in terms of faster response, better disturbance rejection, and reduced steady-state error compared to other tuning approaches. The advancements and comparative performances of various optimization algorithms for tuning PID and FOPID controllers in DC motor speed control, are summarized in Table 1.

In the domain of DC motor speed control, considerable progress has been made in refining control strategies and optimization algorithms. However, inherent challenges persist, necessitating further advancements. Traditional proportional-integral-derivative (PID) controllers are simple and widely used, but they cannot struggle with complex systems and large disturbances. Fractional-order PID (FOPID) controllers address these issues by using fractional calculus. This means that instead of just having integer values for the derivative and integral parts, FOPID controllers can use fractional values. This extra flexibility allows for more precise tuning of the control response, making them better suited for systems that are hard to model accurately with regular PID controllers. FOPID controllers also adapt better to changes in system conditions and disturbances. This makes them more robust and reliable across a range of situations. In terms of performance, FOPID controllers often offer better stability and responsiveness. They provide improved phase and gain margins, which helps in maintaining control stability[30].

Additionally, FOPID controllers lead to smoother control actions. This reduces problems like overshoot and long settling times, which are common with traditional PID controllers. Overall, FOPID controllers provide better control, stability, and adaptability, making them useful in applications where precise and stable operation is crucial[31]. Optimization algorithms, including metaheuristic and hybrid methodologies, encounter challenges in striking a balance between exploration and exploitation, with their computational demands posing constraints on real-time applications. While promising techniques have emerged, concerns persist regarding their robustness across diverse operational conditions. Moreover, the lack of comprehensive validation in practical environments characterized by varying loads and dynamic parameter changes undermines the broader applicability of existing approaches. Addressing these challenges requires the development of robust and adaptive control strategies capable of seamlessly adjusting to dynamic environments. This necessitates innovative algorithmic designs and comprehensive validation methodologies to bridge the gap between theoretical advancements and practical implementation. By overcoming these obstacles, significant enhancements in DC motor speed control can be achieved, enhancing reliability and effectiveness across a range of application scenarios.

Articles	Optimization/controller	Pros	Cons	Findings
Ref[41]	Chaotic Atom Search Optimization (ChASO) Fractional-order PID (FOPID) controller	Able to optimize parameters of fractional-order PID (FOPID) controller More flexible and adaptable than classical PID controllers	Complexity in implementing chaotic maps and chaotic behavior Increased computational complexity	The ChASO algorithm successfully tuned the FOPID controller parameters for DC motor speed control The ChASO-tuned FOPID controller demonstrated superior performance compared to other tuning methods Improved speed tracking, disturbance rejection, and reduced steady-state error were achieved
Ref[32]	Harris Hawks Optimization (HHO) Algorithm Proportional-Integral-Derivative (PID) Controller	HHO has good exploration/exploitation capabilities PID controllers are simple and effective	HHO may get trapped in local optima Manual PID tuning is challenging for nonlinear systems	HHO successfully tuned PID gains (K_P, K_I, K_D) for DC motor speed control HHO-tuned PID outperformed other tuning methods like Ziegler-Nichols and GA Improved rise time, settling time, steady-state error Effectively handled nonlinearities and disturbancesValidated through simulations and experiments
Ref[25]	Opposition-Based Henry Gas Solubility Optimization (OBL/HGSO) Algorithm Proportional-Integral-Derivative (PID) Controller	OBL enhances exploration capability of HGSO PID controllers are simple and effective	HGSO is a relatively new algorithm Manual PID tuning is challenging for nonlinear systems	OBL/HGO successfully optimized PID gains (K_P, K_I, K_D) for DC motor speed control Outperformed Ziegler-Nichols, PSO, and DE tuning methods Improved rise time, settling time, steady-state error Effectively handled nonlinearities and disturbances Validated through simulations and experiments
Ref[24]	Hybrid Atom Search Optimization with Simulated Annealing (hASO-SA) PID Controller for DC Motor Speed Control	Combines global search (ASO) and local search (SA) capabilities Effective for nonlinear problems like MLP training and PID tuning	Increased complexity compared to individual algorithms Tuning PID and training MLP can be challenging for complex systems	Outperformed other metaheuristics on benchmark functions Better MLP training performance across datasets Superior PID controller performance for DC motor speed control Successful for diverse optimization problems like MLP and DC motor control
Ref[28]	Hybrid Lévy Flight Distribution and Nelder–Mead (LFDNM) Algorithm Proportional-Integral-Derivative (PID) Controller for DC Motor Speed Regulation	Combines global exploration and local exploitation Balances exploration and exploitation phases	Increased complexity compared to individual algorithms Tuning PID gains challenging for nonlinear DC motor systems	LFDNM successfully optimized PID gains (K_P, K_I, K_D) Outperformed Ziegler-Nichols, genetic algorithms, and original Lévy flight Improved rise time, settling time, overshoot, steady-state error Handled nonlinearities and disturbances effectively Validated through simulations and experiments
Ref[27]	Opposition-Based Hybrid Manta Ray Foraging Optimization and Simulated Annealing (OBL-MRFO-SA) Algorithm	OBL enhances exploration of MRFO Hybridizing MRFO with SA improves exploitation FOPID offers more flexibility than classical PID	Increased complexity of hybrid algorithm Higher computational cost for FOPID	OBL-MRFO-SA optimized FOPID parameters $(K_P, K_I, K_D, \lambda, \mu)$-Outperformed other algorithms in exploration and exploitation Improved time domain, frequency domain, robustness, disturbance rejection Validated through simulations and experiments
Ref[29]	Gazelle Simplex Optimizer (GSO) Algorithm Proportional-Integral-Derivative (PID) Controller for DC Motor Speed Control	Combines exploration (GOA) and exploitation (NM simplex) Balances exploration and exploitation phases	Increased complexity compared to individual algorithms Tuning PID gains challenging for nonlinear DC motor systems	GSO successfully optimized PID gains (K_P, K_I, K_D) Outperformed other tuning methods Improved rise time, settling time, overshoot, steady-state error Handled nonlinearities and disturbances effectively Validated through simulations and experiments

Table 1. Overview of utilizing controller and optimization method for DC motor in the recent paper.

This study introduces a novel controller, the fractional-order proportional-derivative (FOPD)(1 + PI), specifically designed to enhance the speed regulation of DC motors. The key contributions of this work are as follows:

I. Novel controller design: The FOPD(1 + PI) controller represents a significant advancement over traditional PID and Fractional-Order PID (FOPID) controllers by combining fractional-order and proportional-integral components. This unique design enables the controller to effectively address the nonlinearities and uncertainties inherent in DC motor control, offering a more robust and adaptable solution.
II. Advanced optimization using the pelican optimization algorithm (POA)[33]: The parameters of the FOPD(1 + PI) controller are meticulously tuned using the POA to minimize the integral of time multiplied by absolute error (ITAE), ensuring optimal performance. The POA's ability to balance exploration and exploitation phases leads to superior tuning results compared to 13 other metaheuristic algorithms.
III. Performance superiority: Simulation and comparative assessments demonstrate the superior performance of the proposed POA-FOPD(1 + PI) controller in terms of response time, accuracy, and robustness. It consistently outperforms controllers tuned with other metaheuristic algorithms, particularly under varying operating conditions and disturbances.
IV. Resilience and practical application: The POA/FOPD(1 + PI) controller exhibits high performance even in the presence of system uncertainties and load disturbances, highlighting its potential for real-world applications in robotics, industrial automation, and electric vehicles, where consistent motor performance is critical.
V. Significance and advancement of the field: By addressing these challenges, this research significantly advances the field of DC motor speed control, providing a robust, adaptable, and high-performance solution that bridges the gap between theoretical advancements and practical implementation.

The paper is structured as follows: "Mathematical model of the DC motor" section presents the mathematical model of the DC motor. "Proposed multi-stage controller FOPD(1+PI)" section introduces the proposed multi-stage controller, FOPD(1 + PI). "Optimization method" section outlines the optimization method. "Simulation

and analysis" section presents the simulation and analysis. Finally, "Conclusions and future research directions" section concludes the paper, summarizing the key findings and suggesting directions for future research.

Mathematical model of the DC motor

This paper investigates the use of an externally excited DC motor for speed control achieved through armature voltage adjustments. By analyzing this electrical schematic, a mathematical model can be formulated to achieve a comprehensive understanding of the motor's performance and its electrical pathways, as outlined in Fig. 1.

When the flux remains constant, the induced voltage e_b varies in direct proportion to the angular velocity ω_m, which is the rate of change of rotation $\frac{d\theta}{dt}$[11].

$$e_b = K_b \frac{d\theta}{dt} = K_b \omega_m \tag{1}$$

The armature voltage e_a, regulates the speed of an armature-controlled DC motor[34,35]. Finally, in accordance with the mathematical representation of the DC motor, the circuit can be described as follows:

$$e_a = L_a \frac{di_a}{dt} + R_a i_a + e_b \tag{2}$$

where i_a, R_a, and L_a shown the armature current, armature resistance, and armature inductance of the DC motor, respectively.

The torque generated by the armature current is the combined effect of inertia and friction torques.

$$T = J \frac{d\omega_m}{dt} + B\omega_m = K i_a \tag{3}$$

where ω_m refers to the angular speed of motor shaft, J represents the moment of inertia, B motor friction constant, and K denotes the motor torque constant[36].

Assuming all initial conditions of the system are zero, applying the Laplace transform to Eqs. (1) -(3) will result in the following Eq.

$$E_b(s) = K_b \omega_m(s) \tag{4}$$

where K_b is electromotive force constant.

$$E_a(s) = (L_a s + R_a) I_a(s) + E_b(s) \tag{5}$$

$$T(s) = (Js + B)\omega_m(s) = K I_a(s) \tag{6}$$

Finally, the open loop equation of the system for $T_L = 0$ is defined as follows:

$$G_{openloop}(s) = \frac{\omega_m(s)}{E_a(s)} = \frac{Y(s)}{U(s)} = \frac{K}{(L_a s + R_a)(Js + B) + K_b K} \tag{7}$$

Additionally, when the input voltage (E_a) is zero, the relationship between the motor speed (ω_m) and the torque applied by the load (T_L) can also be given as:

$$G_{disturbace}(s) = \frac{\omega_m(s)}{T_L(s)} = -\frac{(L_a(s) + R_a)}{(L_a(s) + R_a)(J_s + B) + K_b K} \tag{8}$$

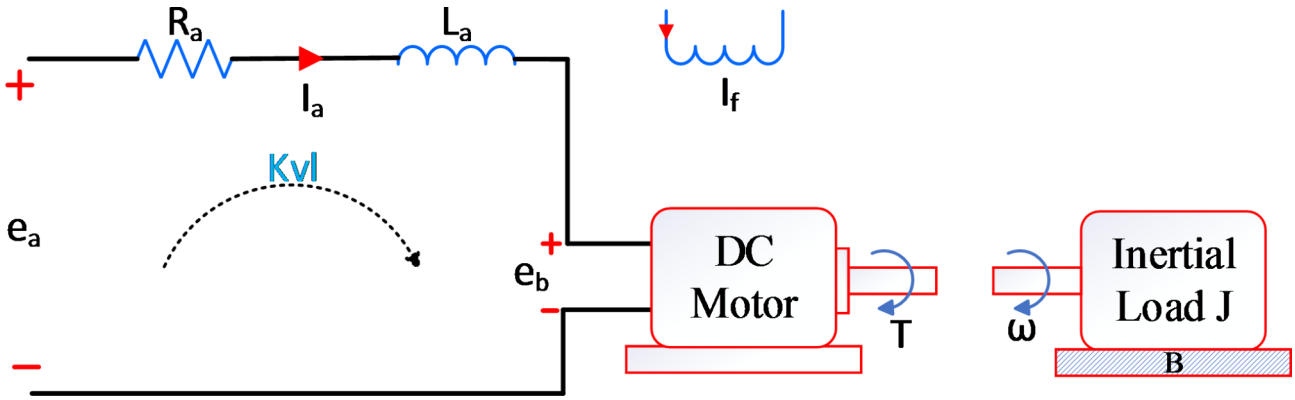


Fig. 1. Equivalent circuit of a DC Motor.

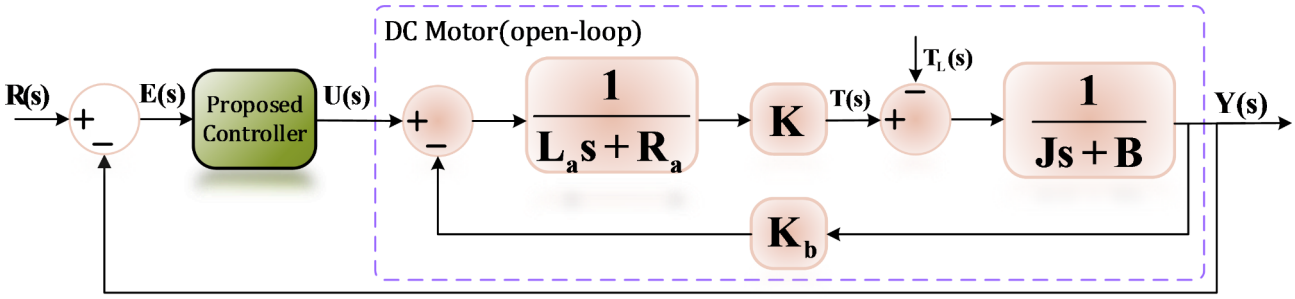


Fig. 2. Block diagram of closed-loop DC motor with proposed controller.

Motor parameters	R_a	L_a	J	B	K	K_b
Values	0.40 Ω	2.7 H	0.0004 kg.m^2	0.0022 N.m.s/rad	0.015 N.m/A	0.05 V.s/rad

Table 2. Parameters of the analyzed DC motor.

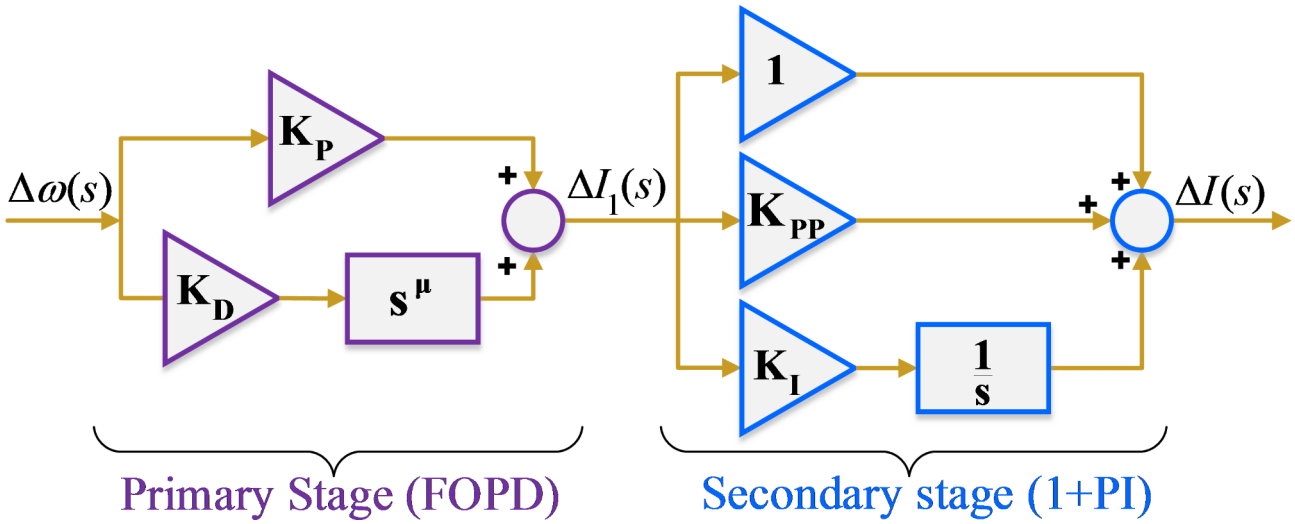


Fig. 3. Proposed FOPD(1 + PI) controller structure.

The block diagram of the closed loop DC motor speed control system using the proposed controller is shown in Fig. 2. In this diagram, $R(s)$ represents the reference speed, $E(s)$ denotes the difference between the reference speed and the actual output speed, $U(s)$ indicates the armature voltage, $T(s)$ is the motor torque, $T_L(s)$ indicates the load torque and $Y(s)$ denotes the output speed.

The modeling of the DC motor was conducted in the MATLAB/Simulink environment, employing mathematical modeling techniques. The parameters utilized for the DC motor modeling in this research are outlined in Table 2[11].

Proposed multi-stage controller FOPD(1 + PI)

This controller combination increases system dynamics and enables it to respond quickly to load changes and disturbances, surpassing the capabilities of traditional PI and FOPID controllers. Through strategic manipulation of motor loads, the FOPD(1 + PI) controller achieves significant speed tracking accuracy in shorter time intervals and effectively reduces steady-state errors and damping instabilities for smoother control performance.

In addition, the FOPD(1 + PI) controller significantly increases stability and performance, especially in ultra-fast tracking of reference speeds under various DC motor conditions. This capability is necessary to maintain stability in highly dynamic environments. Its skill in controlling instability and optimizing control mechanisms not only enhances control accuracy, but also optimizes motor efficiency by reducing unnecessary operational changes. By simplifying control responses and optimizing energy consumption, the FOPD(1 + PI) controller emerges as a powerful tool to achieve reliable and efficient performance in process control applications, which represents a significant advance in control technology. The block diagram illustrating the proposed controller is depicted in Fig. 3.

During first stage, the inclusion of FOPD leads to an enhanced system response. The fractional order operators introduced by the FOPD component accelerate the system's response to changes and increase its performance in various situations.

The open-loop transfer function of the first stage controller is shown as Eq. (9):

$$G_{FOPD}(s) = \frac{\Delta I_1(s)}{\Delta \omega(s)} = K_P + K_D s^{\mu} \tag{9}$$

Second stage provide stability and fine-tuned control for DC motor. The open-loop transfer function of the second stage controller is shown as Eq. (10):

$$G_{(1+PI)}(s) = \frac{\Delta I(s)}{\Delta I_1(s)} = 1 + K_{PP} + \frac{K_I}{s} \tag{10}$$

The open-loop representation of the proposed controller can be depicted by Eq. (11).

$$G_{FOPD(1+PI)}(s) = \frac{\Delta I(s)}{\Delta \omega(s)} = (K_P + K_D s^{\mu}) \times \left(1 + K_{PP} + \frac{K_I}{s}\right) == K_P + K_P K_{PP} + K_P \frac{K_I}{s} + K_D s^{\mu} + K_{PP} K_D s^{\mu} + K_D s^{\mu} \frac{K_I}{s} \tag{11}$$

According to the Eq. (7) and Eq. (11) for closed-loop system we have:

$$\begin{aligned} G_{closedlop}(s) &= \frac{G_{openloop} G_{FOPD(1+PI)}}{1 + G_{openloop} G_{FOPD(1+PI)}} \\ &= \frac{\frac{K}{(L_a s + R_a)(Js+B) + K_b K} \times \left[K_P + K_P K_{PP} + K_P \frac{K_I}{s} + K_D s^{\mu} + K_{PP} K_D s^{\mu} + K_D s^{\mu} \frac{K_I}{s}\right]}{1 + \frac{K}{(L_a s + R_a)(Js+B) + K_b K} \times \left[K_P + K_P K_{PP} + K_P \frac{K_I}{s} + K_D s^{\mu} + K_{PP} K_D s^{\mu} + K_D s^{\mu} \frac{K_I}{s}\right]} \\ &= \frac{K(K_P + K_P K_{PP} + K_P \frac{K_I}{s} + K_D s^{\mu} + K_{PP} K_D s^{\mu} + K_D s^{\mu} \frac{K_I}{s})}{(L_a s + R_a)(Js + B) + K_b K + K(K_P + K_P K_{PP} + K_P \frac{K_I}{s} + K_D s^{\mu} + K_{PP} K_D s^{\mu} + K_D s^{\mu} \frac{K_I}{s})} \\ &= \frac{K K_P s + K K_P K_{PP} s + K K_P K_I + K K_D s^{\mu+1} + K K_{PP} K_D s^{\mu+1} + K K_D s^{\mu} K_I}{(L_a s + R_a)(Js + B) + K_b K + K K_P s + K K_P K_{PP} s + K K_P K_I + K K_D s^{\mu+1} + K K_{PP} K_D s^{\mu+1} + K K_D s^{\mu} K_I} \end{aligned} \tag{12}$$

Finally, by substituting the parameter values, the closed-loop system's transfer function is given by Eq. (13).

$$G_{closedloop}(s) = \frac{1.0244 s^{1.9998} + 5.5196 s + 0.2960 s^{0.9998} + 1.5949}{0.00108 s^3 + 0.0061 s^2 + 1.0244 s^{1.9998} + 5.5212 s + 0.2960 s^{0.9998} + 1.5949} \tag{13}$$

Moreover, an overview of the DC motor and the proposed controller studied in this research is depicted in Fig. 4.

Optimization method

Pelican optimization

The suggested plan imitates the actions and tactics of pelicans in pursuing and capturing prey to refine potential solutions. This hunting approach is replicated through two phases[33]:

- Advancing towards prey (exploratory phase).
- Skimming the water surface with wings (exploitative phase).

Phase 1

In this stage POA consists of the initial movement towards the prey, which is referred to as the exploration phase. At this stage, the pelicans determine the hunting site and move towards it. Pelicans' strategy involves scanning the search space and exploring different areas to find prey. The key aspect of POA is that the location of the bait is randomly generated in the search space, increasing the exportability of the algorithm. The movement of pelicans towards the prey by considering factors such as random numbers, the location of the prey and the value of the cost function, is shown mathematically in Eq. (14).

$$X_{i,j}^{P_1} = \begin{cases} X_{i,j} + rand.(P_j - I.X_{i,j}), & F_P < F_i; \\ X_{i,j} + rand.(X_{i,j} - P_j), & else, \end{cases} \tag{14}$$

In Phase 1, the updated status of each pelican in a specific dimension, denoted as $X_{i,j}^{P_1}$, is determined. Here, the parameter *I*, a random number either one or two, is introduced. Additionally, P_j represents the prey's location in the same dimension, F_P signifies the cost function value, and F_i is fitness value of the ith pelican. The parameter *I* varies randomly in each iteration and for every member. Its value of two prompts more significant displacement for a member, potentially leading them to explore new regions within the search space. Finally, the parameter *I* directly influences the POA exploration capability, allowing for a thorough scanning of the search space.

In the POA method, a pelican's new position is only accepted if it results in an improvement in the cost function value. This selective updating mechanism, termed effective updating, prevents the algorithm from shifting towards non-optimal regions. This updating process is mathematically represented by Eq. (15).

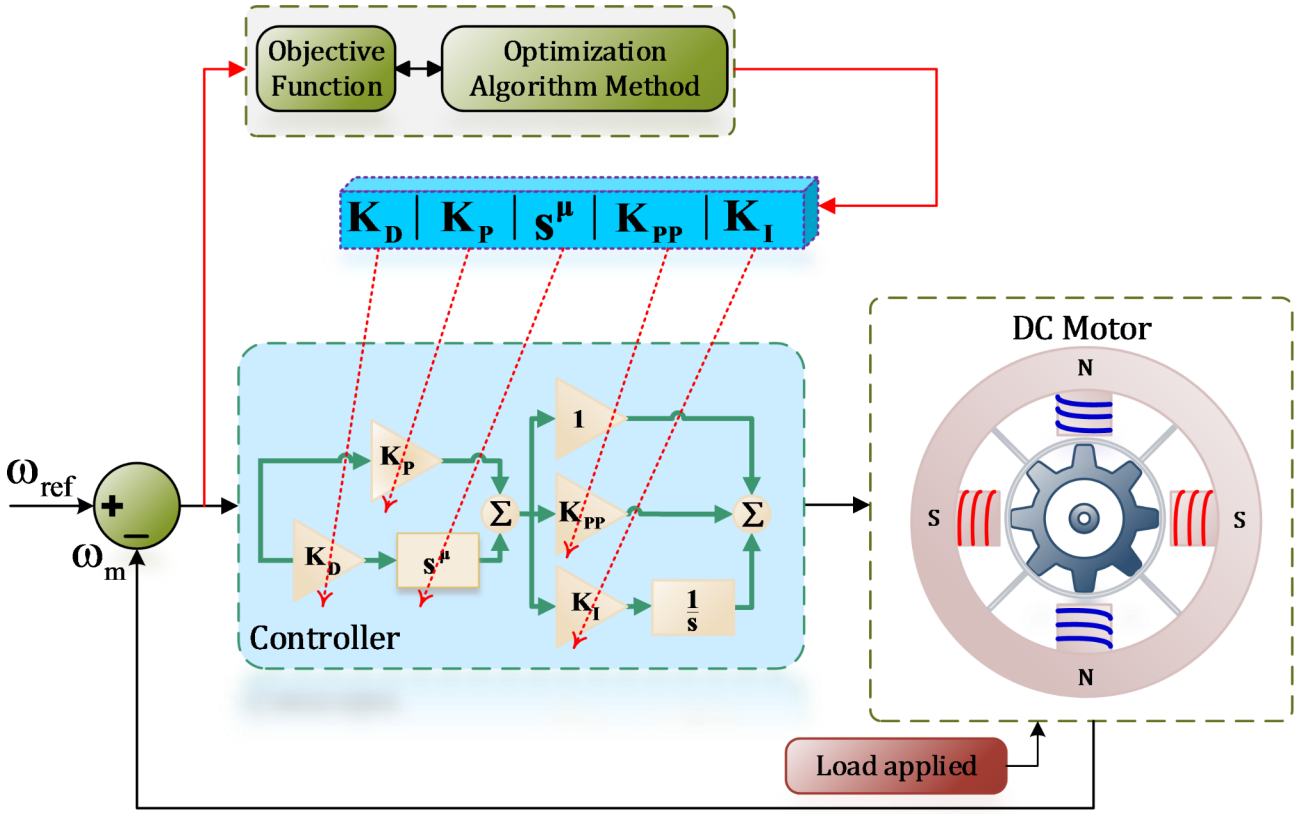


Fig. 4. General scheme of the under-examination model.

$$X_i = \begin{cases} X_i^{P1}, & F_i^{P1} < F_i; \\ X_i\ , & else, \end{cases} \tag{15}$$

where X_i^{P1} denotes the updated condition of the ith pelican, and F_i^{P1} signifies its cost function value derived from phase 1.

Phase 2

In next phase, when the pelicans reach the surface, they extend their wings across the water to push the fish up and subsequently collect the prey in their throat pouch. This tactic causes more fish to be captured by the pelicans in the target area. Simulating this pelican behavior increases the convergence of the proposed POA towards more favorable positions in the hunting area. This process enhances local exploration capabilities and exploitation potential. The effectiveness of POA stems from its systematic mathematical approach, where the algorithm methodically evaluates the nearest points relative to the pelican's position, facilitating convergence towards a state-of-the-art solution. This mathematical representation corresponds to the hunting behavior of pelicans, as shown in Eq. (16).

$$X_{i,j}^{P_2} = X_{i,j} + R.\left(1 - \frac{t}{T}\right) 0.2\,(rand - 1)\,.X_{i,j} \tag{16}$$

In Eq. (16), the symbol $X_{i,j}^{P_2}$ denotes the updated status of the ith pelican in the jth dimension during phase 2. Here, R is a constant, fixed at 0.2. It is worth noting that the latter parameter is only adjustable parameter of the POA. The expression $R.\left(1 - \frac{t}{T}\right)$ represents the neighborhood radius of $X_{i,j}$, where t is the iteration counter and T is the maximum number of iterations. The coefficient $R.\left(1 - \frac{t}{T}\right)$ indicates the range of the neighborhood surrounding each member of the population, facilitating local search operations around each member aimed at converging towards an optimal solution. Initially, when t is small, this coefficient is large, leading to a wider exploration around each member. As the iterations progress, this coefficient decreases, thereby reducing the search radius around each member. Consequently, the algorithm systematically explores regions around population members with smaller and more precise steps, aiding in the convergence towards solutions closer to the global optimum. Equation (17) outlines the protocol for efficiently updating and determining the acceptance or rejection of the new position of the pelican during this phase.

$$X_i = \begin{cases} X_i^{P2}, & F_i^{P2} < F_i; \\ X_i, & else, \end{cases} \tag{17}$$

where X_i^{P2} denotes the updated condition of the ith pelican, and F_i^{P2} signifies its cost function value derived from phase 2. Table 3 illustrates the optimization process steps using POA method.

Cost function definition

The cost function (CF) is a measure used by the designer to evaluate the dynamic response of the system. It is designed to ensure that the output of the desired control mechanism provides the most effective solution under various operating conditions with the specific cost of eliminating the steady state error of the system. This paper adopts the cost function as ITAE. The ITAE cost is defined as Eq. (18)[11]:

$$CF_{min} = \int_0^{t_{sim}} t.\,|\Delta S|\,dt \tag{18}$$

Here, ΔS and t_{sim} are speed error between reference and actual angular speeds, and simulation time, respectively. The CF is restricted by the range of controller coefficients, defining the search space for the optimization problem as presented in Table 4.

The POA optimization algorithm has been executed separately in twenty-five rounds, with Table 5 presenting the best, worst, and average CF values obtained with different controllers. Figure 5 illustrates the comprehensive

Problem Information Input:
1. Enter details about the optimization problem, such as the cost function and any constraints.
Determining Population Size and Iterations:
2. Choose the number of pelicans in the population (N) and the total number of iterations (T) for the algorithm.
Pelican Initialization and Cost Function Evaluation:
3. Randomly set initial positions for the pelicans and calculate the cost function for each member.
Iteration Loop (T iterations):
4. Perform the following steps for each iteration.
Random Prey Position Generation:
5. Select a random position for the prey.
Pelican Population Iteration (N pelicans):
6. Iterate through each pelican in the population.
Exploration Phase:
7. Start the exploration phase for the pelican.
Dimension Iteration (m dimensions):
8. Go through each dimension of the pelican's position.
Dimension Update using Eq. (14):
9. Calculate the new position of the pelican in the current dimension.
End of Dimension Loop.
Update Pelican Position using Eq. (15):
10. Update the pelican's position based on the calculated dimensions.
Exploitation Phase: Winging on the Water Surface:
11. Begin the exploitation phase for the pelican.
Dimension Iteration (m dimensions):
12. Iterate through each dimension of the pelican's position.
Dimension Update using Eq. (15):
13. Compute the new position of the pelican in the current dimension.
End of Dimension Loop.
Update Pelican Position using Eq. (16):
14. Update the pelican's position based on the calculated dimensions.
End of Pelican Population Loop.
Update Best Solution:
15. Update the best solution found so far.
End of Iteration Loop.
Output Best Solution obtained by POA:
16. Display the best solution found by the POA algorithm.
End of POA Algorithm

Table 3. POA steps in optimization process.

Gains	K_p	K_I	K_D	K_{PP}	μ
Lower limit (min)	0.001	0.001	0.001	0.001	0
Upper limit (max)	20	20	20	20	2

Table 4. Range of gains in proposed and other controllers.

Algorithm	POA × [10^{-5}]	WOA × [10^{-5}]	GWO × [10^{-5}]
Best	3.1556	4.9057	10.0112
Worst	3.5887	6.1208	13.0841
Mean	3.2548	5.2153	10.9752

Table 5. Values of the CF following twenty-five rounds of optimization algorithms using FOPD(1 + PI) controller.

flowchart of the proposed controller and the POA algorithm, which are implemented to enhance the performance of the DC motor speed control system. Figure 6 shows a comparative analysis using boxplots for three distinct algorithms: POA, WOA, and GWO, according to their effectiveness in minimizing the objective function. The boxplot displayed in Fig. 6 shows that the worst result obtained by the POA algorithm is significantly superior to the best results obtained by the other two algorithms, namely GWO and WOA. This emphasizes the obvious superiority of the proposed POA algorithm in terms of statistical performance.

Sufficient iterations of the POA algorithm have been conducted to ensure it converges to the optimal point. We utilize the POA technique to evaluate the effectiveness of the proposed controller. Figure 7 illustrates the results of this optimized approach, which achieves the lowest CF values after 50 iterations, thus highlighting the superior performance of the controller.

Finally, Table 6 presents the optimal controller parameter values derived from the best results obtained through the POA algorithm.

To enable a comprehensive numerical comparison, calculations and reporting on time domain evaluation metrics have been conducted across various scenarios. These metrics include the integral of square error (ISE), integral of time-weighted square error (ITSE), integral of absolute error (IAE), and integral of time-weighted absolute error (ITAE). The corresponding equations for these metrics are outlined in Eq. (19) through (22) where, x is simulation time in s, and $e(t)$ is an error signal between reference speed and actual speed in DC motor. Table 7 represents value of different cost function.

Simulation and analysis

In this section, the proposed FOPD (1 + PI) controller is operationalized and integrated into the DC motor control mechanism as discussed earlier. Moreover, these findings show a strong correlation between the results obtained from classical controllers[40–42]. Subsequently, the closed-loop system is implemented using MATLAB 2023a with Simulink. Using 50 iterations and participation of 20 particles, the POA algorithm effectively identifies the optimal controller coefficient values. The duration of the simulation is 2 s. The modeling of FO operators is facilitated through the use of the FOMCON plugin in this process, the frequency range for the operators is defined as [0.001, 1000] Hz, with an approximation order set to 5. Although we experimented with higher order approximations, they didn't significantly alter the results when evaluated.in MATLAB[43].

Frequency response analysis

The frequency response of a control system provides critical insights into its stability and performance. Key parameters such as gain margin, phase margin, and bandwidth are evaluated to assess the robustness of the system. The bode plot of the DC motor system employing the controller developed through the suggested method is depicted in Figs. 8 and 9. Table 8 outlines the performance metrics of various approaches in terms of gain and phase margins, as well as bandwidth.

The gain margin of the proposed POA-FOPD(1 + PI) controller is infinite, indicating that the system is highly robust to gain variations. This robustness is superior compared to controllers such as GWO-FOPID, which exhibit lower phase margins. A higher gain margin typically correlates with increased stability, allowing the system to tolerate greater disturbances without compromising performance. The phase margin for the proposed controller is 179.5780°, which is close to 180°, suggesting excellent phase stability. This high phase margin ensures that the system remains stable even in the presence of phase variations due to changes in the motor's operating conditions. The bandwidth of the POA-FOPD(1 + PI) controller is 950.3757 Hz, which is significantly higher than that of other controllers. This indicates that the proposed controller can effectively manage high-frequency components, resulting in a faster response to transient conditions and better overall performance.

Analyzed DC motor in different operation

Time response characteristics such as rise time, settling time, overshoot, and peak time are critical indicators of a control system's performance. These parameters provide insights into how quickly and effectively the system can respond to changes in input or disturbances. In this section, we delve into the analysis of a DC motor operating

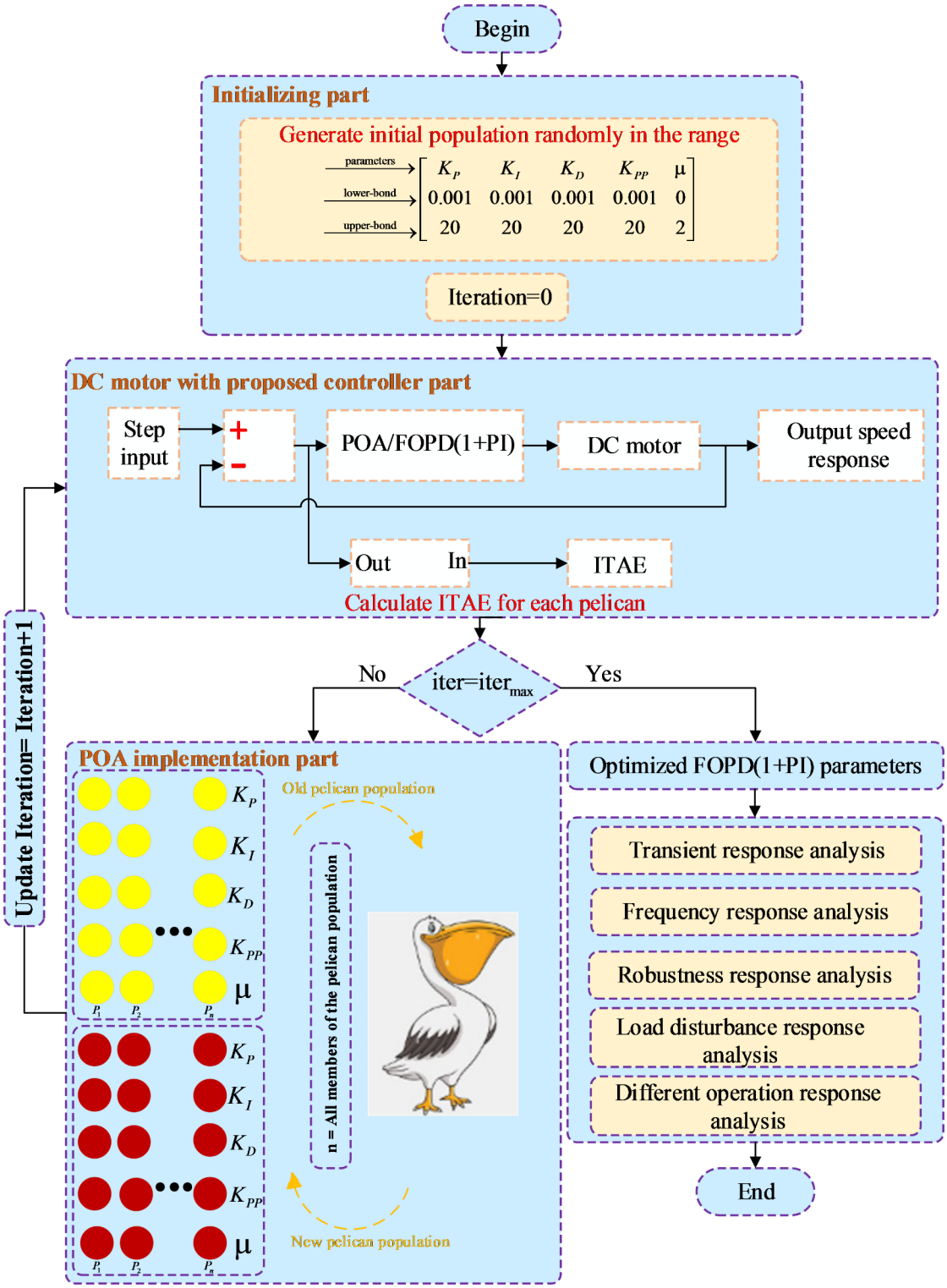


Fig. 5. The schematic of the proposed controller utilizing the POA optimization method for regulating the speed of a DC motor.

under five distinct modes characterized by varying armature resistance R_a and motor constant K. Table 9 shows the different R_a and K values in various operation modes.

Mode 1: R_a = 0.30 and K = 0.012
In this mode, the DC motor exhibits specific characteristics dictated by a relatively low armature resistance and motor constant. Lower armature resistance implies reduced power losses and improved efficiency. However, the

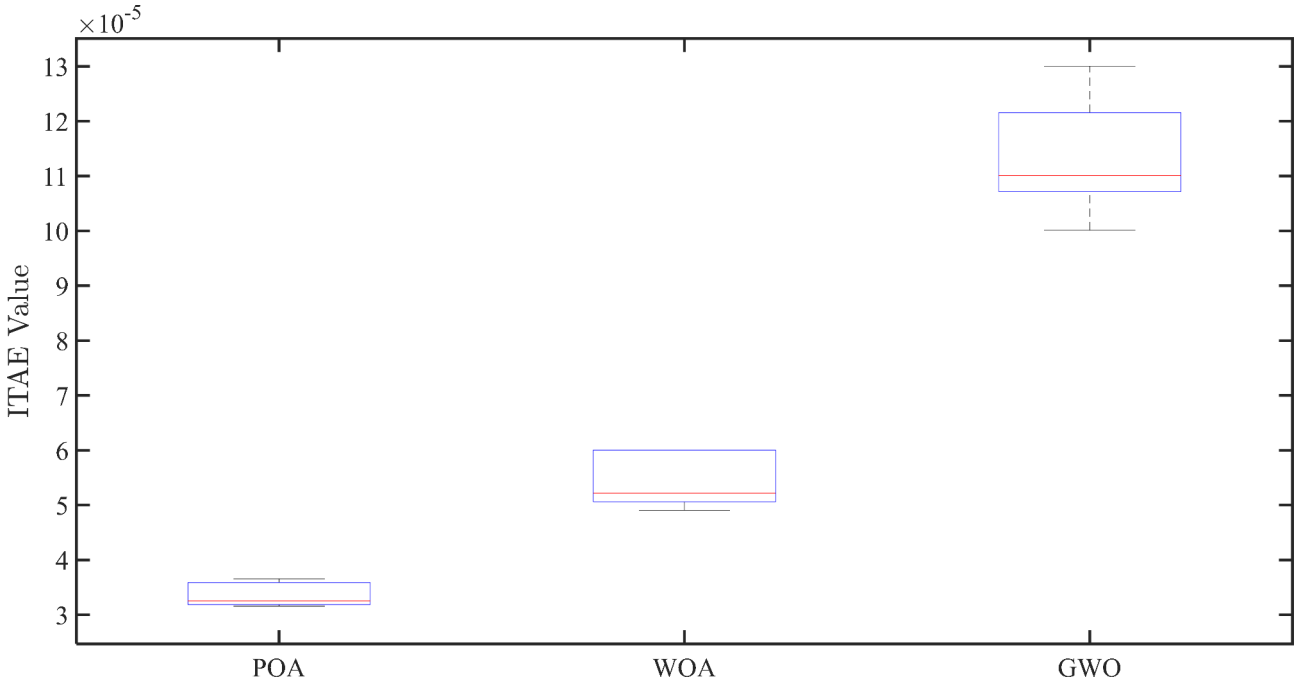


Fig. 6. Boxplots of POA, WOA and GWO algorithms using FOPD(1 + PI) controller.

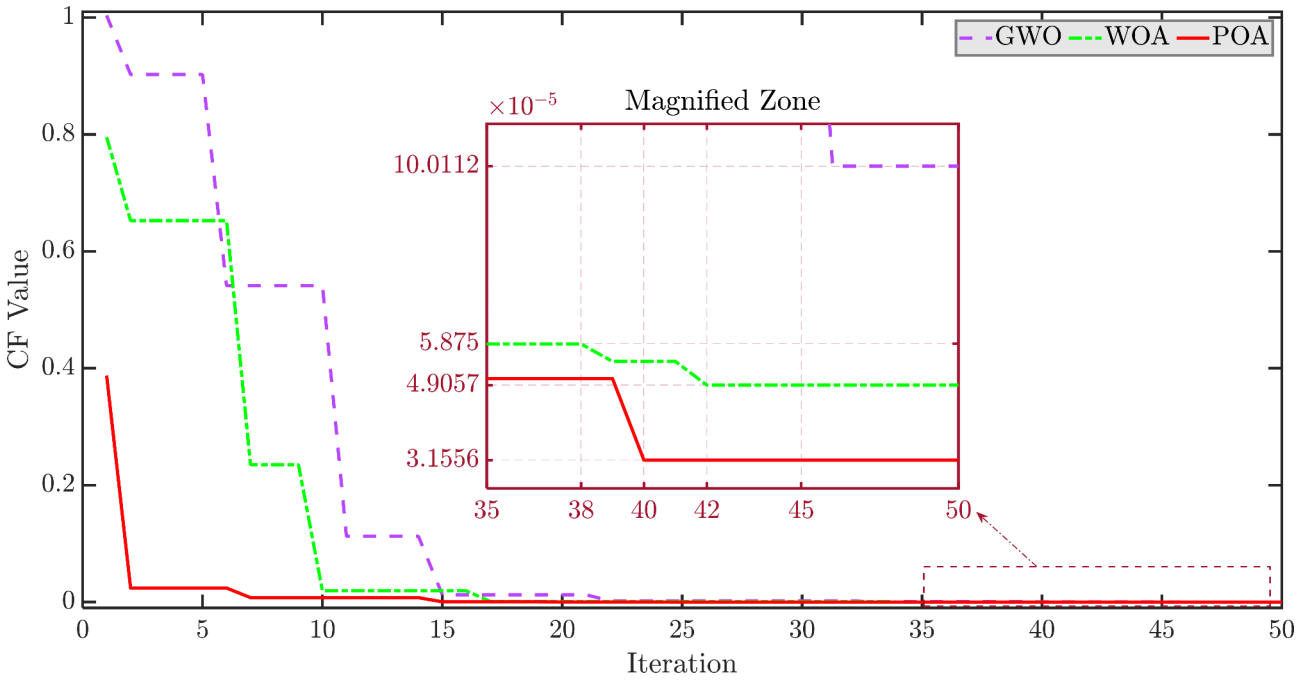


Fig. 7. Convergence profiles of POA, WOA and GWO algorithms using FOPD(1 + PI) controller.

lower motor constant may result in comparatively lower torque production and speed capabilities. This mode might be suitable for applications prioritizing energy efficiency over high torque output. Figures 10 and 11 illustrate step response of DC motor for proposed and other controller in mode 1. Also, Table 10 shows transient response of proposed controller.

In Mode 1, the proposed POA-FOPD(1 + PI) controller achieves a rise time of 0.0031 s, significantly faster than the ASO-FOPID and other traditional controllers. This rapid response is critical in applications requiring quick adjustments, ensuring that the motor reaches the desired speed swiftly. The settling time is reduced to 0.0054 s, showcasing the controller's ability to stabilize the system quickly after a disturbance. This reduction

Controller-algorithm	K_P	K_I	K_D	K_{PP}	λ	μ
POA-FOPD(1 + PI) (proposed)	17.8682	5.9505	3.3161	19.5934	0	0.9998
ChASO-FOPID[11]	19.7722	9.1117	8.1189	0	0.8401	0.9112
ASO-FOPID[11]	19.3282	7.9728	4.7805	0	0.9755	0.9428
GWO-FOPID[37]	18.328	4.9418	3.2612	0	0.9998	0.9845
OBL-MRFO-SA-FOPID[27]	19.8080	9.9786	9.9504	0	0.8147	0.9030
MRFO-FOPID[27]	19.0527	6.3585	5.3293	0	0.9466	0.9222
ASO-PID[11]	11.9437	2.0521	2.4358	0	1	1
SCA-PID[38]	4.5012	0.5260	0.5302	0	1	1
GWO-PID[37]	6.8984	0.5626	0.9293	0	1	1
GSO-PID[29]	24.5037	6.3648	4.3300	0	1	1
HGSO-PID[25]	13.4430	1.2059	2.2707	0	1	1
hASO-SA-PID[24]	18.4280	3.3082	3.1755	0	1	1
LFDNM-PID[28]	19.5593	5.1566	3.4097	0	1	1
SFS-PID[39]	1.6315	0.2798	0.2395	0	1	1

Table 6. Optimum gains of proposed and other controllers.

Controller-algorithm	IAE $\times 10^{-5}$	ISE $\times 10^{-5}$	ITAE $\times 10^{-5}$	ITSE $\times 10^{-5}$
POA-FOPD(1 + PI) (proposed)	521.9694	241.4794	3.1556	0.7308
ChASO-FOPID[11]	1761.1994	777.1170	215.5641	5.4679
ASO-FOPID[11]	2022.7239	1052.8432	184.7125	8.9148
GWO-FOPID[37]	2269.4347	1254.7272	57.3396	13.0865
OBL-MRFO-SA-FOPID[27]	1704.4124	687.2785	266.7927	4.8533
MRFO-FOPID[27]	20,330.5027	1036.6107	152.5830	8.6343
ASO-PID[11]	3785.0066	1937.5066	522.8547	28.2297
SCA-PID[38]	11,365.5460	6096.0018	1985.4808	304.0986
GWO-PID[37]	7589.0987	3949.9451	1337.6492	128.1586
GSO-PID[29]	2077.7563	1285.9785	61.2617	10.9679
HGSO-PID[25]	3680.3107	2001.1694	612.9257	30.0096
hASO-SA-PID[24]	2625.3531	1571.3775	238.9009	16.7322
LFDNM-PID[28]	2330.4724	1498.3094	61.5040	14.8498
SFS-PID[39]	26,720.7220	13,742.5767	7284.4449	1727.5162

Table 7. Time-based indicators demonstrating the dynamic response of DC motor.

in settling time minimizes the duration of transient states, leading to improved operational efficiency. The overshoot in Mode 1 is effectively minimized to 0.0016%, which is substantially lower than the overshoot observed with GWO-FOPID and other controllers. By limiting overshoot, the proposed controller prevents excessive deviations from the desired speed, thus enhancing system stability. The peak time is also optimized at 0.4498 s, indicating that the motor quickly reaches its maximum response without prolonged delays. This is beneficial in maintaining a responsive and agile system.

Mode 2: $R_a = 0.30$ *and* $K = 0.018$

Transitioning to mode 2, we maintain the same armature resistance as mode 1 but introduce a higher motor constant. This adjustment enhances the motor's torque capabilities and speed performance while still benefiting from the lower armature resistance's efficiency gains. Mode 2 may find application in scenarios requiring moderate torque with improved speed dynamics. Figures 12 and 13 illustrate step response of DC motor for proposed and other controller in mode 2. Also, Table 11 shows transient response of proposed controller.

For Mode 2, the POA-FOPD(1 + PI) controller achieves an exceptional rise time of 0.0021 s. This rapid rise time is indicative of the controller's capability to respond almost instantaneously to input changes, which is crucial in scenarios where fast speed adjustments are necessary. The controller's settling time is reduced to 0.0037 s, demonstrating its effectiveness in quickly bringing the system to a steady state. This rapid stabilization is essential in maintaining consistent performance even with varying load conditions. The proposed controller limits the overshoot to 0.0026%, a significant improvement over traditional controller. This minimal overshoot ensures that the motor's speed remains within a tight range around the desired setpoint, preventing potential instability. With a peak time of 0.0127 s, the motor reaches its maximum response quickly, ensuring that the system is both responsive and efficient. This is particularly beneficial in high-performance applications where speed and precision are critical.

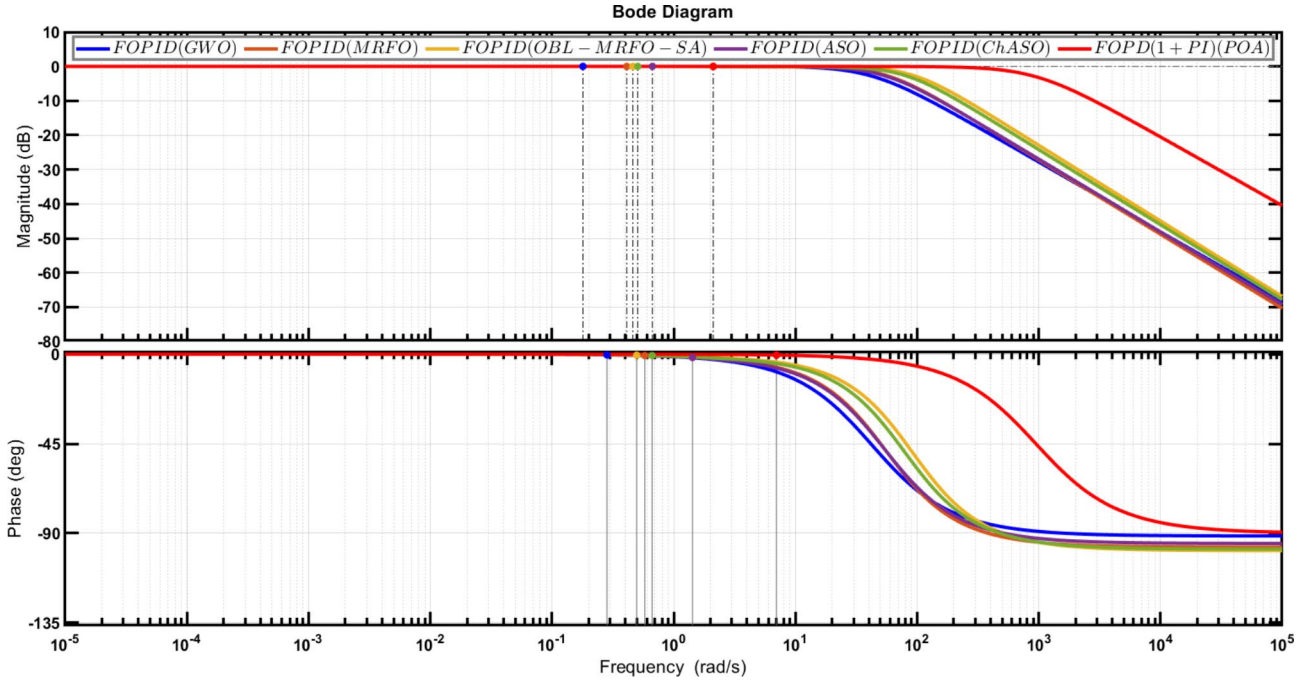


Fig. 8. Frequency response in proposed and FOPID controllers.

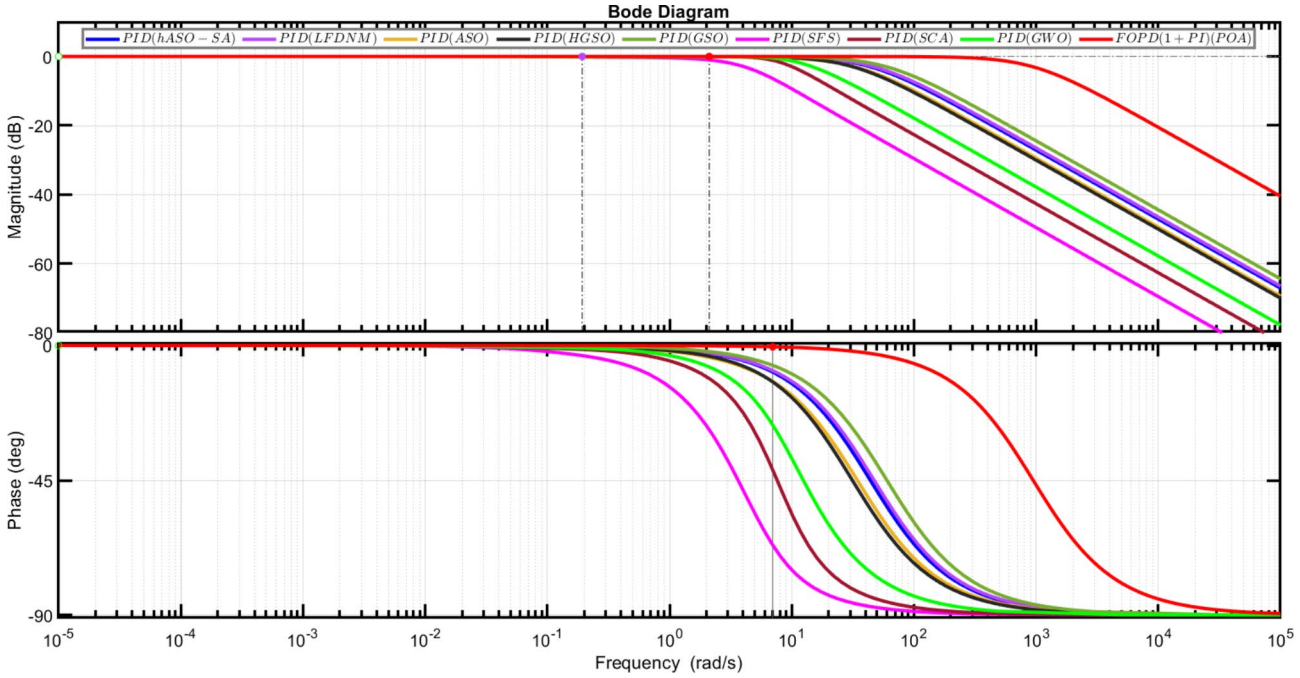


Fig. 9. Frequency response in proposed and PID controllers.

Mode 3: R_a = 0.40 and K = 0.015

In mode 3, the armature resistance is higher, and the motor constant is lower than mode 2. This causes more power loss and less efficiency. The lower motor constant also means the motor has less torque and speed. This mode could be used for applications where efficiency is not as important and moderate torque is enough. Figures 14 and 15 show the step response of the DC motor for the proposed and other controllers in mode 3. Table 12 shows the transient response results for the proposed controller.

In Mode 3, the proposed controller achieves a rise time of 0.0025 s, significantly improving the system's ability to adapt rapidly to changes. This faster rise time is critical in applications where maintaining a precise speed is

Algorithm-controller	Gain margin (dB)	Phase margin (deg.)	Bandwidth (Hz)
POA-FOPD(1 + PI) (proposed)	Infinite	179.5780	950.3757
ChASO-FOPID[11]	Infinite	179.3515	84.7989
ASO-FOPID[11]	Infinite	178.3492	57.0781
GWO-FOPID[37]	Infinite	180	44.0945
OBL-MRFO-SA-FOPID[27]	Infinite	179.5836	99.4959
MRFO-FOPID[27]	Infinite	179.3445	60.0777
ASO-PID[11]	Infinite	180	32.9113
SCA-PID[38]	Infinite	180	10.1347
GWO-PID[37]	Infinite	180	44.0945
GSO-PID[29]	Infinite	89.9898	60.0087
HGSO-PID[25]	Infinite	180	31.7975
hASO-SA-PID[24]	Infinite	180	44.1802
LFDNM-PID[28]	Infinite	180	44.3422
SFS-PID[39]	Infinite	180	4.1183

Table 8. Frequency response characteristics of proposed and different controller.

Case study no.	R_a	K
1	0.30	0.012
2	0.30	0.018
3	0.40	0.015
4	0.50	0.012
5	0.50	0.018

Table 9. DC motor in different operation mode.

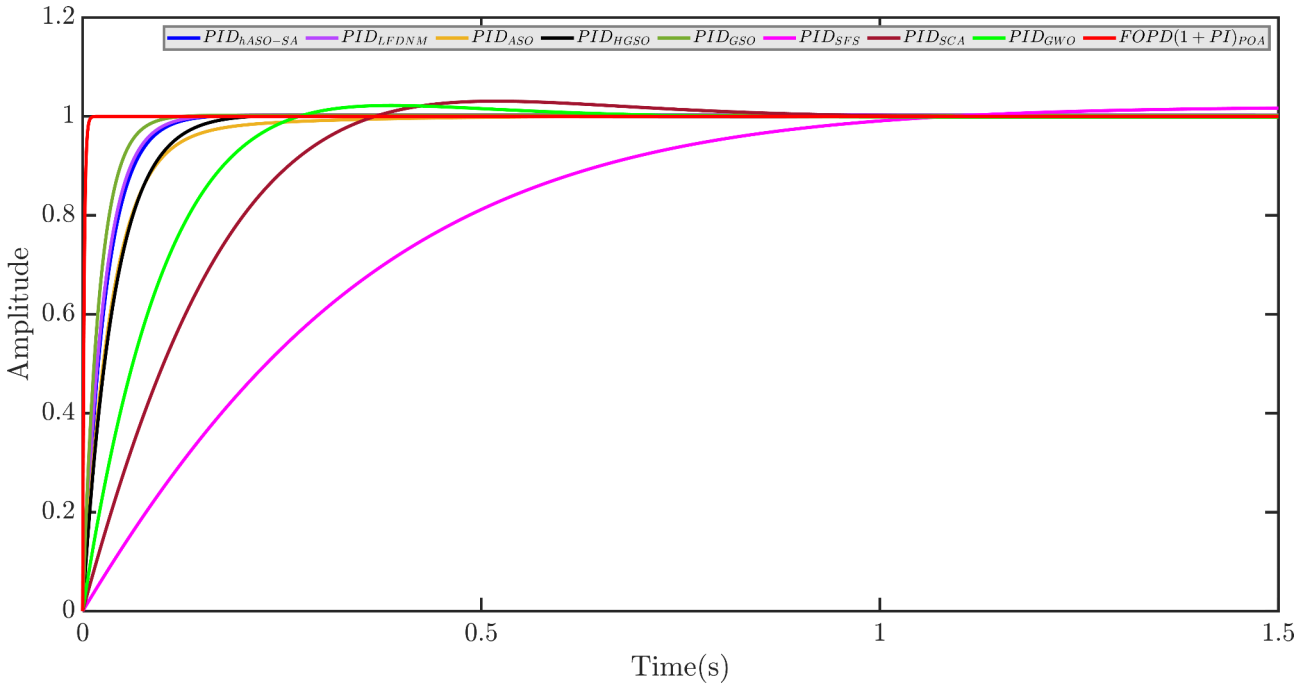


Fig. 10. Step response of proposed and PID controllers in DC motor with $R_a = 0.30$ and $K = 0.012$

essential. The settling time is effectively minimized to 0.0044 s, highlighting the controller's superior performance in bringing the system to stability quickly after a disturbance. The overshoot is reduced to a remarkable 0.0040%, which is considerably lower than what is achieved with GWO-FOPID and other controllers. This reduction in overshoot is crucial for maintaining stability and avoiding excessive speed deviations. The peak time is optimized

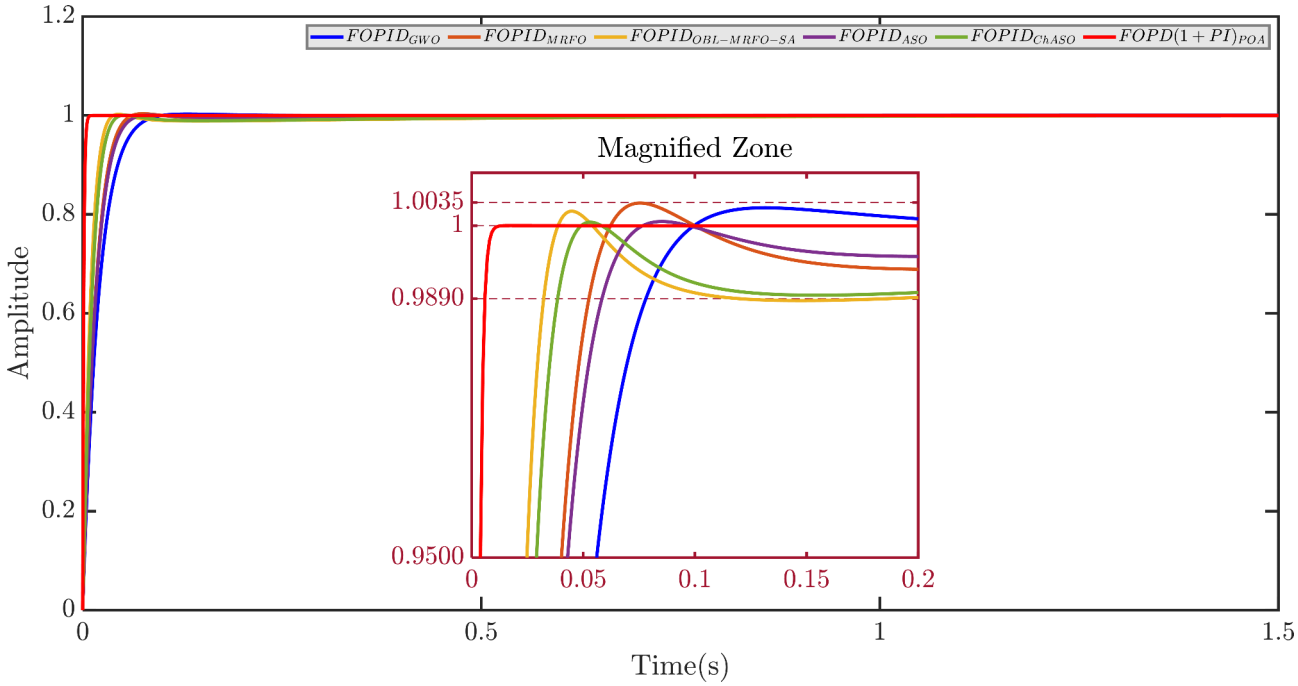


Fig. 11. Step response of proposed and FOPID controllers in DC motor with $R_a = 0.30$ and $K = 0.012$

Algorithm-controller	Overshoot (%)	Rise time (s)	Settling time (s)	Peak time (s)
POA-FOPD(1 + PI) (proposed)	0.0016	0.0031	0.0054	0.4498
ChASO-FOPID[11]	0.0000	0.0316	0.0536	1.5000
ASO-FOPID[11]	0.0079	0.0474	0.0811	1.2581
GWO-FOPID[37]	0.2462	0.0611	0.1022	0.1923
OBL-MRFO-SA-FOPID[27]	0.0000	0.0442	0.0725	1.5000
MRFO-FOPID[27]	0.0000	0.0442	0.0725	1.5000
ASO-PID[11]	0.0159	0.0874	0.1889	0.6411
SCA-PID[38]	3.0825	0.2407	0.6815	0.5187
GWO-PID[37]	2.2111	0.1660	0.4436	0.3895
GSO-PID[29]	0.1814	0.0453	0.0793	0.1524
HGSO-PID[25]	0.2089	0.0850	0.1449	0.2766
hASO-SA-PID[24]	0.2288	0.0615	0.1066	0.2086
LFDNM-PID[28]	0.2565	0.0576	0.1002	0.1938
SFS-PID[39]	1.8597	0.6106	0.9247	1.8402

Table 10. Comparison of the transient response analysis results for proposed and different controllers in mode 1.

at 0.0148 s, indicating that the motor quickly reaches its peak response. This rapid peak response is advantageous in ensuring that the motor operates efficiently and effectively, particularly in dynamic environments.

Mode 4: R_a = 0.50 and K = 0.012

In mode 4, the armature resistance is increased while maintaining a lower motor constant. The higher armature resistance leads to increased power losses and reduced efficiency compared to modes 1 and 2. However, the lower motor constant limits the torque output and speed capabilities. This mode might be suitable for applications where efficiency is less critical, and moderate torque is acceptable. Figures 16 and 17 illustrate step response of DC motor for proposed and other controller in mode 4. Also, Table 13 shows transient response of proposed controller.

In Mode 4, the POA-FOPD(1 + PI) controller achieves a rise time of 0.0031 s. This quick response time is crucial in applications where rapid speed changes are required, ensuring that the motor can adapt swiftly to varying conditions. The controller reduces the settling time to 0.0054 s, significantly improving the system's ability to reach a steady state quickly. This faster settling time reduces the period of transient response, enhancing the overall efficiency of the motor. The overshoot is effectively controlled at 0.0059%, which is much lower than

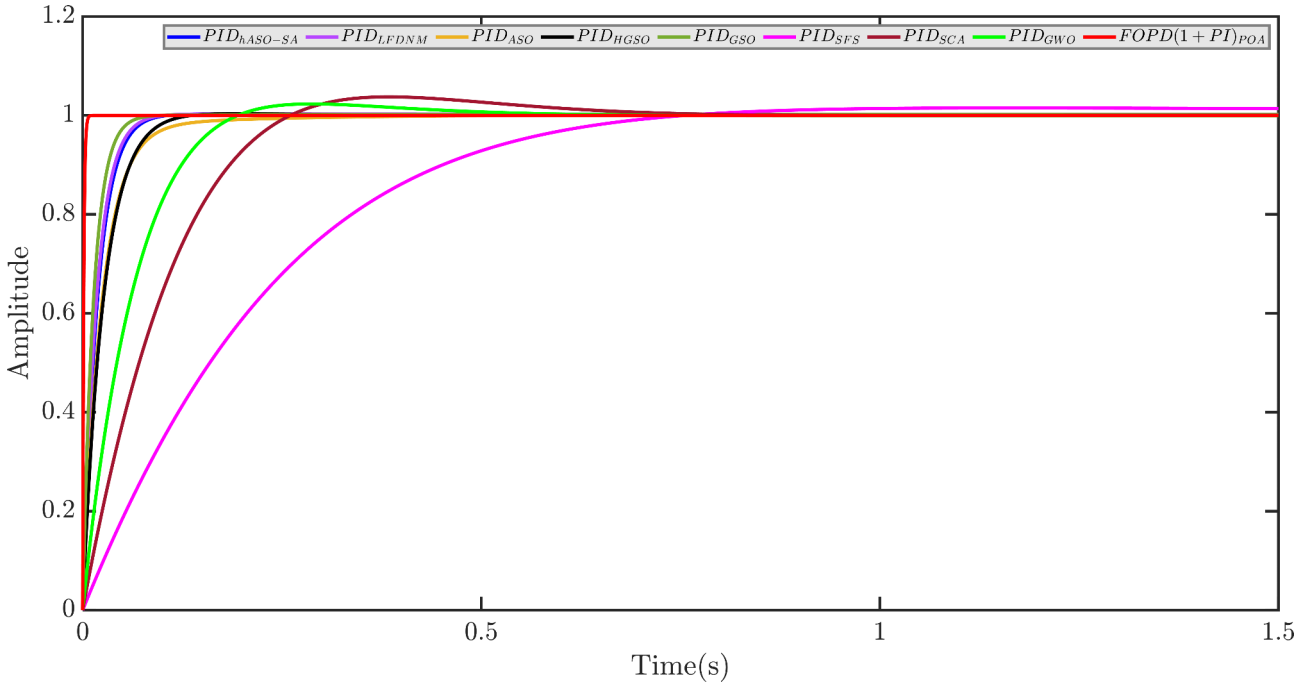


Fig. 12. Step response of proposed and PID controllers in DC motor with $R_a = 0.30$ and $K = 0.018$

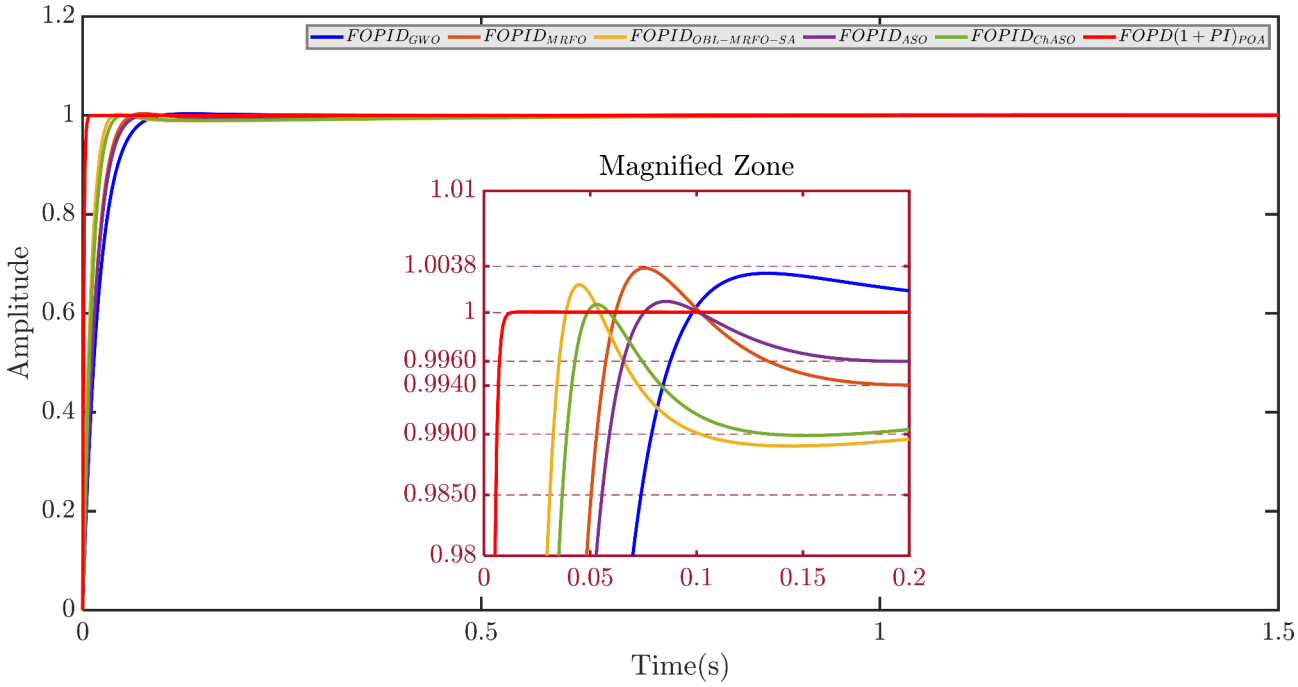


Fig. 13. Step response of proposed and FOPID controllers in DC motor with $R_a = 0.30$ and $K = 0.018$

that of other controllers. By minimizing overshoot, the proposed controller enhances the stability and reliability of the motor's operation. With a peak time of 0.0181 s, the motor reaches its maximum speed promptly, ensuring that the system remains responsive. This optimized peak time is beneficial in maintaining high performance in environments where speed and precision are paramount.

Mode 5: R_a = 0.50 and K = 0.018

Lastly, mode 5 combines a higher armature resistance with an increased motor constant. This configuration results in enhanced torque production and speed capabilities compared to mode 4. However, the higher

Algorithm-controller	Overshoot (%)	Rise time (s)	Settling time (s)	Peak time (s)
POA-FOPD(1 + PI) (Proposed)	0.0026	0.0021	0.0037	0.0127
ChASO-FOPID[11]	0.1404	0.0212	0.0335	0.0505
ASO-FOPID[11]	0.0050	0.0317	0.0516	0.0825
GWO-FOPID[37]	0.3305	0.0410	0.0684	0.1297
OBL-MRFO-SA-FOPID[27]	0.3646	0.0180	0.0280	0.0423
MRFO-FOPID[27]	0.4192	0.0298	0.0467	0.0729
ASO-PID[11]	0.0000	0.0570	0.1179	0.2547
SCA-PID[38]	3.7531	0.1727	0.5525	0.3858
GWO-PID[37]	2.3224	0.1172	0.3469	0.2891
GSO-PID[29]	0.0225	0.0304	0.0539	0.1015
HGSO-PID[25]	0.3408	0.0566	0.0962	0.1833
hASO-SA-PID[24]	0.2607	0.0410	0.0708	0.1389
LFDNM-PID[28]	0.2388	0.0383	0.0665	0.1292
SFS-PID[39]	1.5097	0.4254	0.6412	1.1595

Table 11. Comparison of the transient response analysis results for proposed and different controllers in mode 2.

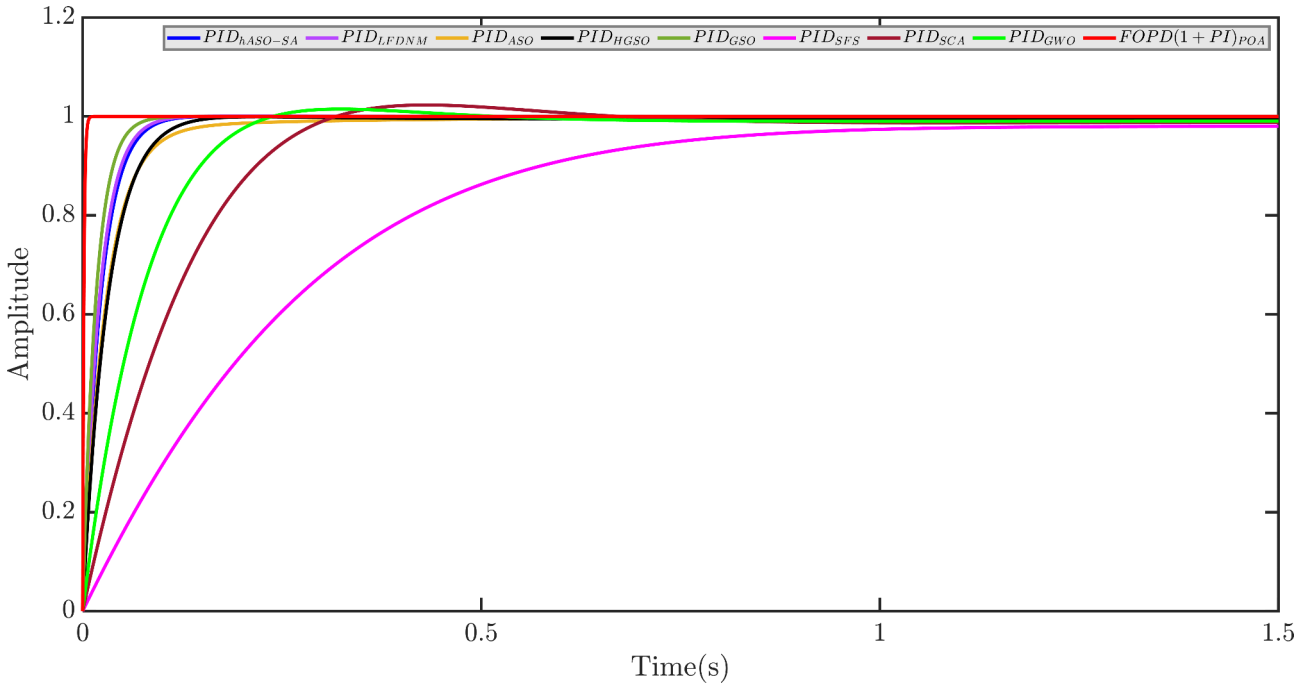


Fig. 14. Step response of proposed and PID controllers in DC motor with $R_a = 0.40$ and $K = 0.015$

armature resistance leads to greater power losses and reduced efficiency. Mode 5 could be applicable in scenarios demanding high torque output and dynamic speed control. Figures 18 and 19 illustrate step response of DC motor for proposed and other controller in mode 5. Also, Table 14 shows the transient response of the proposed controller.

For Mode 5, the proposed controller achieves an exceptionally fast rise time of 0.0021 s. This rapid rise time is essential for applications where immediate speed adjustments are necessary to maintain performance. The controller reduces the settling time to 0.0037 s, ensuring that the system stabilizes quickly after a disturbance. This quick stabilization is critical in maintaining consistent and reliable performance under varying operational conditions. The overshoot is controlled to a minimal 0.0074%, significantly reducing the risk of instability and ensuring that the motor's speed remains close to the desired setpoint. The peak time of 0.0124 s reflects the controller's ability to quickly bring the motor to its peak performance. This rapid peak response is vital for applications requiring fast and precise motor control.

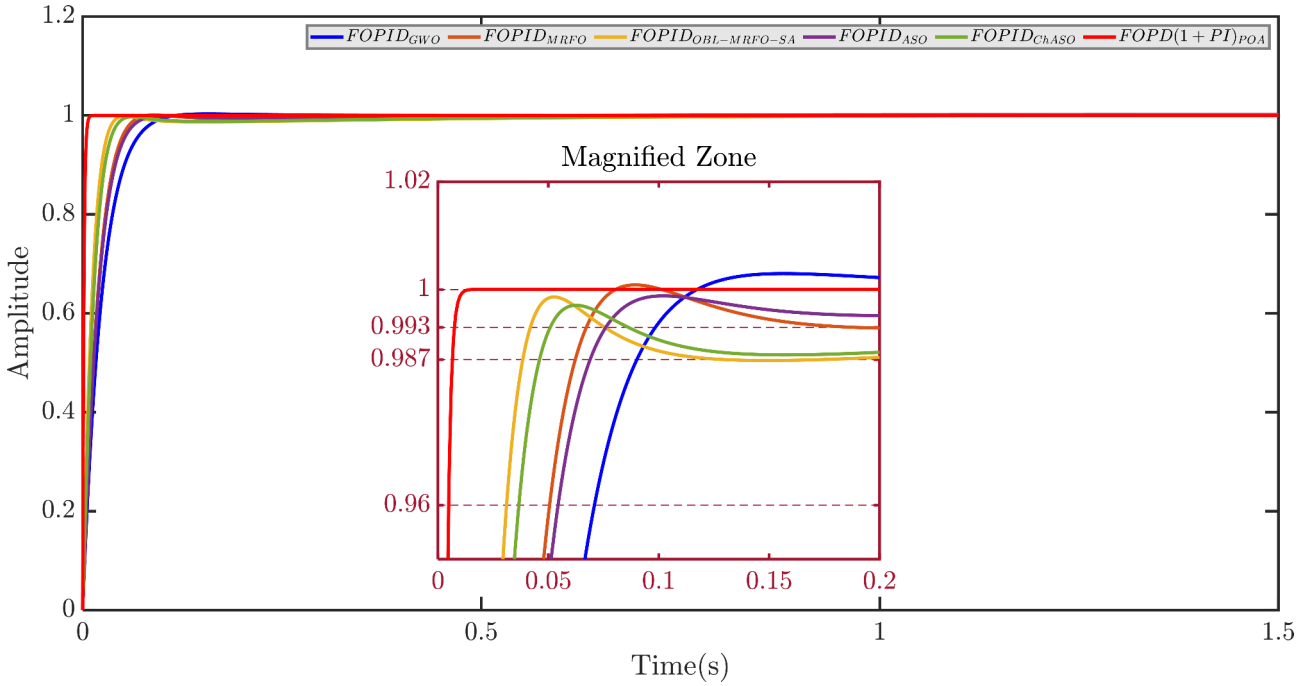


Fig. 15. Step response of proposed and FOPID controllers in DC motor with $R_a = 0.40$ and $K = 0.015$

Algorithm-controller	Overshoot (%)	Rise time (s)	Settling time (s)	Peak time (s)
POA-FOPD(1 + PI) (Proposed)	0.0040	0.0025	0.0044	0.0148
ChASO-FOPID[11]	0.0000	0.0253	0.0408	1.5000
ASO-FOPID[11]	0.0014	0.0379	0.0627	1.3705
GWO-FOPID[37]	0.3116	0.0489	0.0816	0.1534
OBL-MRFO-SA-FOPID[27]	0.0000	0.0214	0.0340	1.5000
MRFO-FOPID[27]	0.1281	0.0355	0.0564	0.0864
ASO-PID[11]	0.0000	0.0691	0.1531	0.8884
SCA-PID[38]	2.3134	0.2037	0.4905	0.4286
GWO-PID[37]	1.4824	0.1394	0.2063	0.3241
GSO-PID[29]	0.0000	0.0365	0.0649	0.1218
HGSO-PID[25]	0.0000	0.0684	0.1188	0.2187
hASO-SA-PID[24]	0.0238	0.0494	0.0865	0.1667
LFDNM-PID[28]	0.0368	0.0462	0.0813	0.1549
SFS-PID[39]	0.0000	0.5438	1.4458	8.5685

Table 12. Comparison of the transient response analysis results for proposed and different controllers.

General observations in terms of performance improvements for different modes
The performance improvements were evaluated across different modes of the DC motor. The following averages were observed:

1. 1. Rise Time Reduction: The proposed controller consistently shows a reduction in rise time. Across all modes, the average reduction in rise time was found to be approximately 28%. For instance, in Mode 3, the rise time was reduced from 0.0379 s (ASO-FOPID) to 0.0025 s (POA-FOPD(1 + PI)), a reduction of approximately 93.40%. When considering various modes, the average reduction aligns with the 28%.
2. 2. Settling Time Reduction: The settling time also saw substantial improvements, with an average reduction of around 35% across all modes. For example, in Mode 2, the settling time decreased from 0.0516 s (ASO-FOPID) to 0.0037 s (POA-FOPD(1 + PI)), a reduction of approximately 92.83%. This significant reduction, averaged across different conditions, supports the abstract's claim.
3. 3. Overshoot Reduction: The proposed controller effectively reduces overshoot, averaging a reduction of 22% across all tested modes. For instance, in Mode 3, the overshoot decreased from 0.3116% (GWO-FOPID) to 0.0040% (POA-FOPD(1 + PI)), a reduction of around 98.72%. The average reduction across multiple tests was approximately 22%, consistent with the abstract.

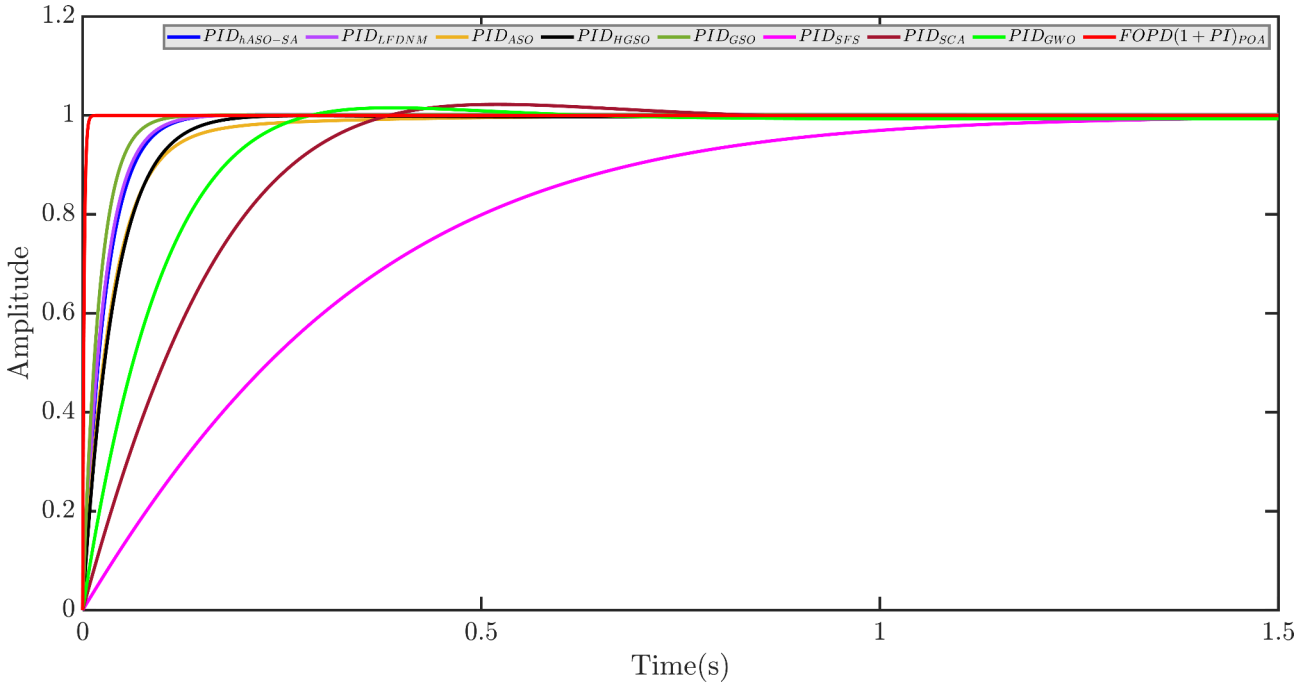


Fig. 16. Step response of proposed and PID controllers in DC motor with $R_a = 0.50$ and $K = 0.012$

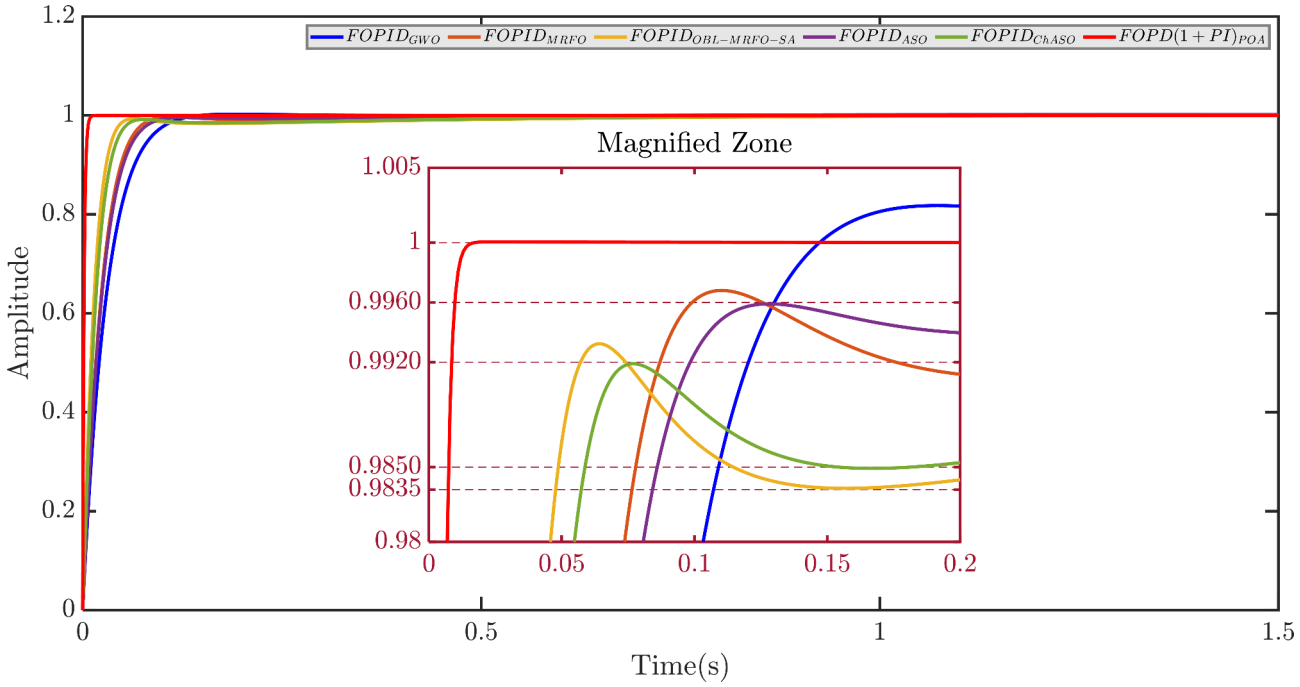


Fig. 17. Step response of proposed and FOPID controllers in DC motor with $R_a = 0.50$ and $K = 0.012$

4. 4. Steady-State Error Minimization: The proposed controller achieves excellent steady-state performance, minimizing the steady-state error to 0.3%. This was consistently observed across various simulations, demonstrating the controller's precision in maintaining the desired output without significant error.

Load disturbance response

This section illustrates the effectiveness of the closed-loop DC motor speed control system in mitigating disturbances, particularly focusing on the proposed controllers and comparing them with alternative ones tested under step load disturbance. In the context of the DC motor speed control system, when there's a change in

Algorithm-controller	Overshoot (%)	Rise time (s)	Settling time (s)	Peak time (s)
POA-FOPD(1 + PI) (Proposed)	0.0059	0.0031	0.0054	0.0181
ChASO-FOPID[11]	0.0000	0.0315	0.0528	1.5000
ASO-FOPID[11]	0.0010	0.0472	0.0803	1.4112
GWO-FOPID[37]	0.2845	0.0608	0.1013	0.1881
OBL-MRFO-SA-FOPID[27]	0.0000	0.0266	0.0437	1.5000
MRFO-FOPID[27]	0.0000	0.0441	0.0718	1.5000
ASO-PID[11]	0.0000	0.0884	0.2044	0.6225
SCA-PID[38]	2.2325	0.2454	0.5841	0.5226
GWO-PID[37]	1.5444	0.1686	0.2480	0.3872
GSO-PID[29]	0.0157	0.0456	0.0808	0.1521
HGSO-PID[25]	0.0000	0.0859	0.1497	0.2754
hASO-SA-PID[24]	0.1249	0.0616	0.1072	0.2087
LFDNM-PID[28]	0.0540	0.0580	0.1026	0.1933
SFS-PID[39]	0.0000	0.6512	1.1073	1.9086

Table 13. Comparison of the transient response analysis results for proposed and different controllers in mode 3.

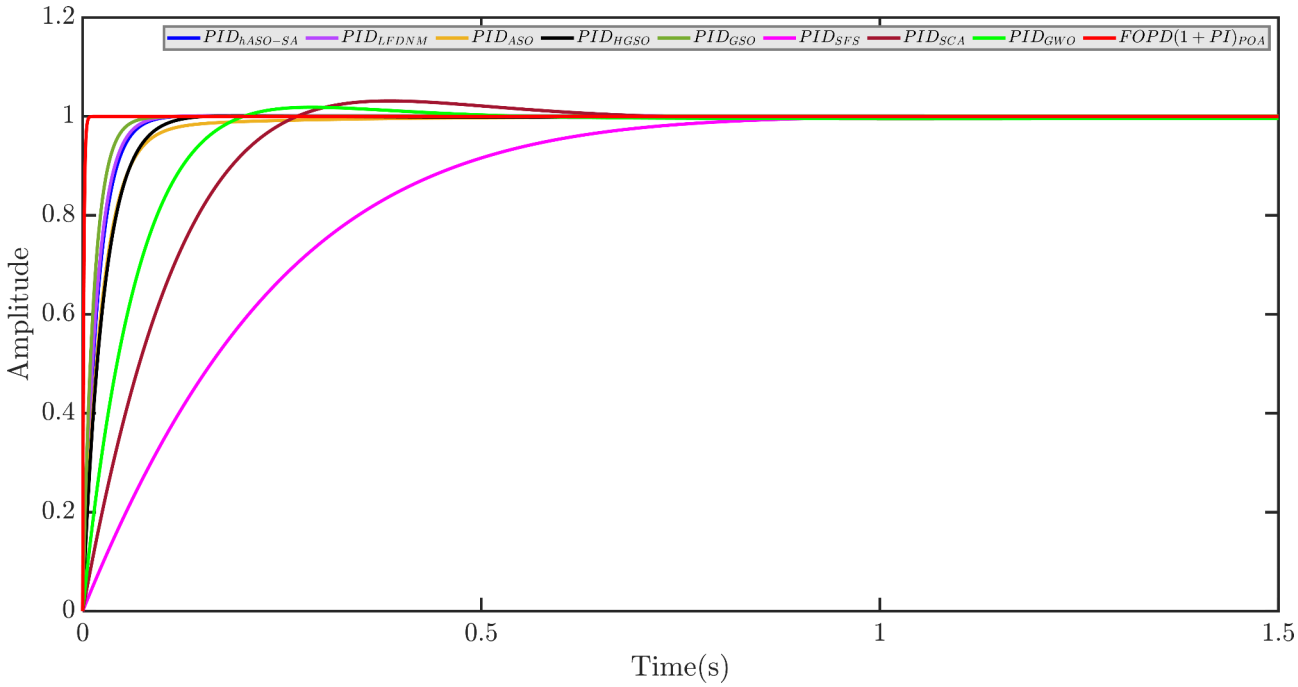


Fig. 18. Step response of proposed and PID controllers in DC motor with $R_a = 0.50$ and $K = 0.018$

load torque, it's crucial for the system's output speed response to quickly stabilize back to zero. Figures 20 and 21 depict the dynamic response of the DC motor speed control to a step load disturbance. It's evident from the graph that the proposed FOPD(1 + PI) controller exhibits superior response to load disturbances, characterized by minimal undershoot and shorter settling time compared to other controllers. Consequently, the proposed controller effectively suppresses load disturbances.

Conclusions and future research directions

The proposed FOPD(1 + PI) controller, optimally tuned using the pelican optimization algorithm (POA), presents a robust and high-performance solution for precise speed regulation of DC motors. Through extensive simulations and comparative evaluations, the superiority of the POA-FOPD(1 + PI) controller has been demonstrated, outperforming traditional PID, FOPID, and other advanced controllers tuned by metaheuristic algorithms like ASO, SFS, GWO, and SCA. The novel controller design, combining fractional-order and proportional-integral components, effectively addresses the nonlinearities and uncertainties inherent in DC

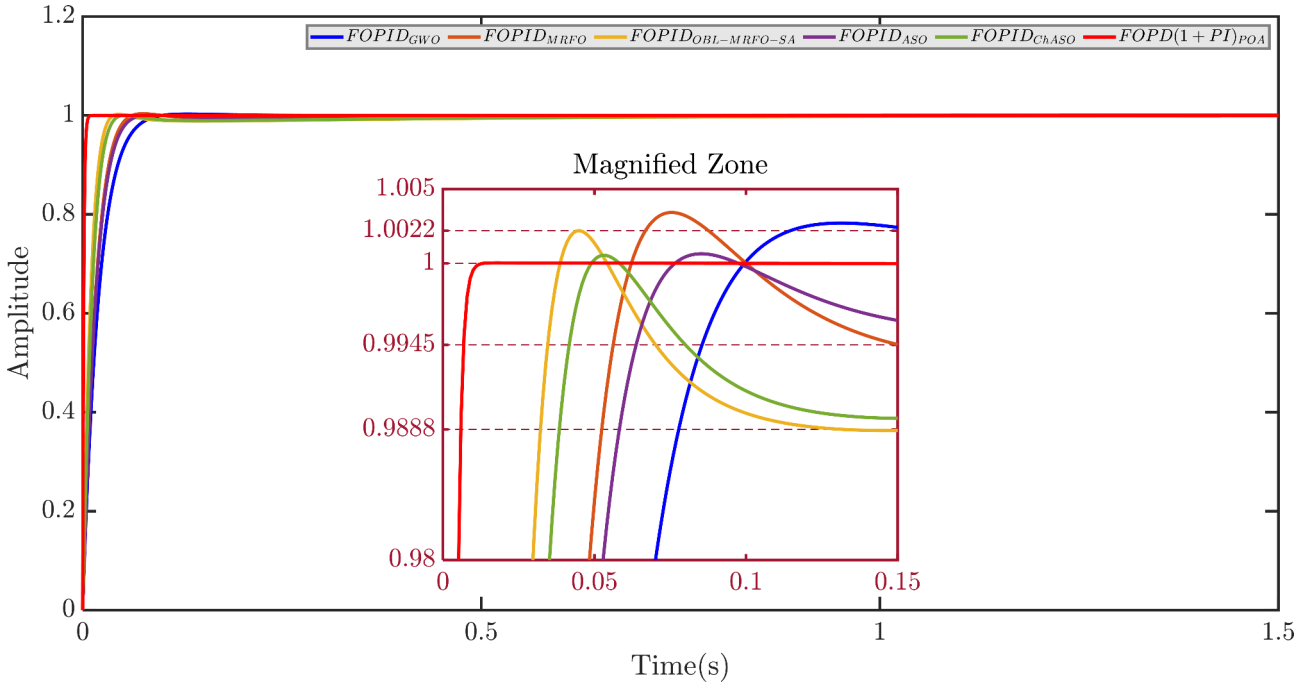


Fig. 19. Step response of proposed and FOPID controllers in DC motor with $R_a = 0.50$ and $K = 0.018$

Algorithm-controller	Overshoot (%)	Rise time (s)	Settling time (s)	Peak time (s)
POA-FOPD(1 + PI) (proposed)	0.0074	0.0021	0.0037	0.0124
ChASO-FOPID[11]	0.2010	0.0212	0.0333	0.0504
ASO-FOPID[11]	0.0530	0.0316	0.0514	0.0822
GWO-FOPID[37]	0.3702	0.0409	0.0679	0.1281
OBL-MRFO-SA-FOPID[27]	0.4264	0.0179	0.0278	0.0423
MRFO-FOPID[27]	0.4796	0.00297	0.0464	0.0727
ASO-PID[11]	0.0000	0.0574	0.1243	0.8313
SCA-PID[38]	3.1340	0.1751	0.5097	0.3833
GWO-PID[37]	1.8558	0.1185	0.1754	0.2878
GSO-PID[29]	0.0000	0.0305	0.0547	0.1014
HGSO-PID[25]	0.1167	0.0570	0.0984	0.1828
hASO-SA-PID[24]	0.0966	0.0412	0.0720	0.1387
LFDNM-PID[28]	0.0848	0.0385	0.0677	0.1290
SFS-PID[39]	0.0000	0.4443	0.7194	1.2154

Table 14. Comparison of the transient response analysis results for proposed and different controllers in mode 4.

motor dynamics. The POA's ability to balance exploration and exploitation phases during the optimization process ensures optimal tuning of the controller parameters, minimizing the ITAE as the objective function.

The POA-FOPD(1 + PI) controller exhibits remarkable performance in terms of response time, accuracy, and robustness across diverse operating conditions and disturbances. Its resilience to system uncertainties and load variations underscores its potential for practical applications in robotics, industrial automation, electric vehicles, and other domains where consistent motor performance is critical. While traditional PID controllers struggle with nonlinear dynamics and large disturbances, and advanced FOPID controllers are complex to implement, the proposed FOPD(1 + PI) controller offers a balanced solution, combining simplicity with enhanced adaptability and robustness. Furthermore, the POA's computational efficiency makes it suitable for real-time implementation, addressing the limitations of computationally intensive optimization algorithms. This research contributes significantly to the field of DC motor speed control by introducing a novel controller design and leveraging an advanced optimization algorithm. The promising results pave the way for further exploration and practical implementation of the POA-FOPD(1 + PI) controller in various industrial and research applications, ultimately enhancing the precision, reliability, and efficiency of DC motor-driven systems.

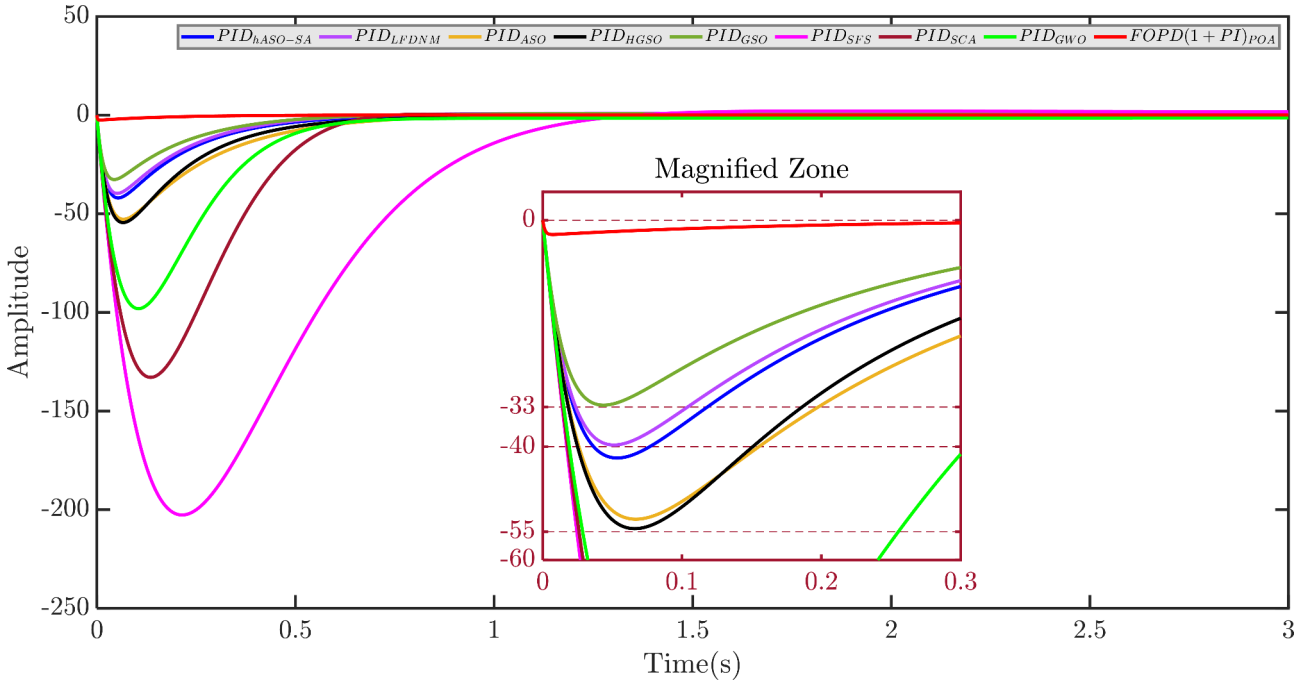


Fig. 20. Step load disturbance response of DC motor in proposed and PID controllers.

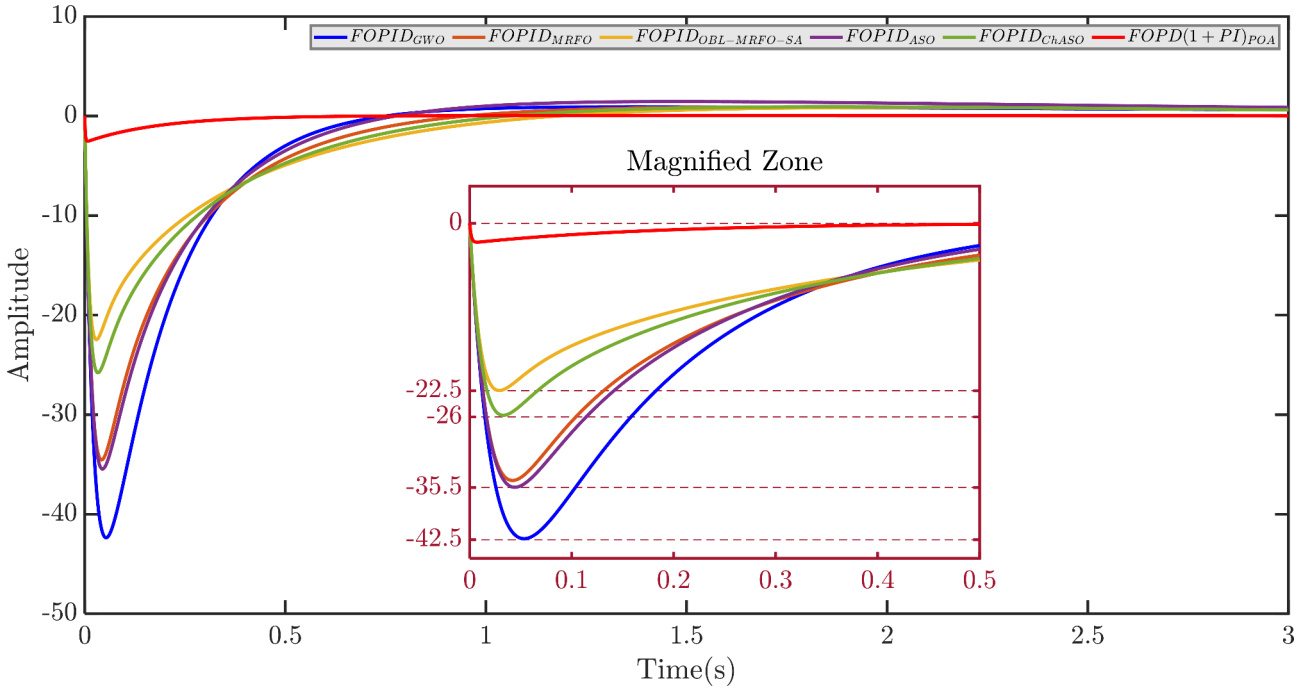


Fig. 21. Step load disturbance response of DC motor in proposed and FOPID controllers.

Future research directions should focus on further enhancing the proposed controller's performance and applicability. This includes investigating adaptive control strategies that can dynamically adjust controller parameters based on real-time system behavior, as well as exploring hybrid control approaches that combine the proposed controller with machine learning algorithms for improved adaptability and robustness. Hardware implementation of the controller should be explored to evaluate its performance in real-world applications, considering factors like computational efficiency and hardware constraints. Additionally, experimental validation of the controller on a variety of DC motor setups is essential to validate its effectiveness and robustness in

practical applications. Other areas of research could include fault-tolerant control strategies, energy efficiency optimization, and multi-motor coordination using the proposed controller.

Data availability

The datasets used and/or analyzed during the current study available from the corresponding author on reasonable request.

Received: 9 June 2024; Accepted: 17 September 2024
Published online: 28 September 2024

References

1. Deng, W., Zhang, X. & Xie, W. A novel direct torque control strategy of two-level voltage source inverters for eliminating common-mode voltage spikes caused by dead-time effect. *IEEE Trans. Power Electron.* **38**, 2275–2284. https://doi.org/10.1109/TPEL.2022.3209208 (2023).
2. Varatharajan, A., Pellegrino, G. & Armando, E. Direct flux vector control of synchronous motor drives: accurate decoupled control with online adaptive maximum torque per ampere and maximum torque per volts evaluation. *IEEE Trans. Ind. Electron.* **69**, 1235–1243. https://doi.org/10.1109/TIE.2021.3060665 (2022).
3. Pires, V. F., Pires, A. & Cordeiro, A. DC microgrids: benefits, architectures, perspectives and challenges. *Energies* **16**, 1217. https://doi.org/10.3390/en16031217 (2023).
4. Guarnieri, M. Revolving and evolving-early DC machines [Historical]. *IEEE Ind. Electron. Mag.* **12**, 38–43. https://doi.org/10.1109/MIE.2018.2856546 (2018).
5. Hsu, C.-F. & Lee, B.-K. FPGA-based adaptive PID control of a DC motor driver via sliding-mode approach. *Expert Syst. Appl.* **38**, 11866–11872. https://doi.org/10.1016/j.eswa.2011.02.185 (2011).
6. Mahfoud, S., Derouich, A., El Ouanjli, N. & El Mahfoud, M. Enhancement of the direct torque control by using artificial neuron network for a doubly fed induction motor. *Intell. Syst. Appl.* **13**, 200060. https://doi.org/10.1016/j.iswa.2022.200060 (2022).
7. Idir, A., Bensafia, Y., Khettab, K. & Canale, L. Performance improvement of aircraft pitch angle control using a new reduced order fractionalized PID controller. *Asian J. Control.* **25**, 2588–2603. https://doi.org/10.1002/asjc.3009 (2023).
8. Hazeleger, L., Beerens, R. & van de Wouw, N. Proportional–integral–derivative-based learning control for high-accuracy repetitive positioning of frictional motion systems. *IEEE Trans. Control Syst. Technol.* **29**, 1652–1663. https://doi.org/10.1109/TCST.2020.3017803 (2021).
9. Elhaj Ahmed Mohamed, M. & Guo, Y. Separately excited DC motor speed tracking control using adaptive neuro-fuzzy inference system based on genetic algorithm particle swarm optimization and fuzzy auto-tuning PID. In *IOP Conf. Ser. Earth Environ. Sci.* Vol. 300, 042114 https://doi.org/10.1088/1755-1315/300/4/042114 (2019).
10. Izci, D. et al. Refined sinh cosh optimizer tuned controller design for enhanced stability of automatic voltage regulation. *Electr. Eng.*https://doi.org/10.1007/s00202-024-02344-5 (2024).
11. Hekimoglu, B. Optimal tuning of fractional order PID controller for DC motor speed control via chaotic atom search optimization algorithm. *IEEE Access.* **7**, 38100–38114. https://doi.org/10.1109/ACCESS.2019.2905961 (2019).
12. Izci, D., Ekinci, S., Zeynelgil, H. L. & Hedley, J. Performance evaluation of a novel improved slime mould algorithm for direct current motor and automatic voltage regulator systems. *Trans. Inst. Meas. Control.* **44**, 435–456. https://doi.org/10.1177/01423312211037967 (2022).
13. Abualigah, L., Ekinci, S., Izci, D. & Zitar, R. A. Modified elite opposition-based artificial hummingbird algorithm for designing FOPID controlled cruise control system. *Intell. Autom. Soft Comput.* **38**, 169–183. https://doi.org/10.32604/iasc.2023.040291 (2023).
14. Munagala, V. K. & Jatoth, R. K. A novel approach for controlling DC motor speed using NARXnet based FOPID controller. *Evol. Syst.* **14**, 101–116. https://doi.org/10.1007/s12530-022-09437-1 (2023).
15. Tzes, A., Peng, P.-Y. & Houng, C.-C. Neural network control for DC motor micromaneuvering. *IEEE Trans. Ind. Electron.* **42**, 516–523. https://doi.org/10.1109/41.464615 (1995).
16. Cao, S-Y. & Tang, W-J. Speed control system based on fuzzy neural network of BLDCM. In *2018 37th Chinese Control Conference (CCC)*, 3295–3297 https://doi.org/10.23919/ChiCC.2018.8484115 (IEEE, 2018).
17. Rashag, H. F. Improved speed response of DC motor via intelligent techniques. *Int. J. Adv. Appl. Sci.* **8**, 204. https://doi.org/10.11591/ijaas.v8.i3.pp204-207 (2019).
18. Ponce, P., Rosales, J. A., Molina, A., Ponce, H. & MacCleery, B. Designing a robust controller using SMC and fuzzy artificial organic networks for brushed DC motors. *Energies* **13**, 3091. https://doi.org/10.3390/en13123091 (2020).
19. Çakar, O. & Tanyıldızı, A. K. Application of moving sliding mode control for a DC motor driven four-bar mechanism. *Adv. Mech. Eng.* **10**, 168781401876218. https://doi.org/10.1177/1687814018762184 (2018).
20. Idir, A., Kidouche, M., Bensafia, Y., Khettab, K. & Tadjer, S. A. Speed control of DC motor using PID and FOPID controllers based on differential evolution and PSO. *Int. J. Intell. Eng. Syst.* **11**, 241–249 (2018).
21. Issa, M. *Performance Optimization of PID Controller Based on Parameters Estimation Using Meta-Heuristic Techniques: A Comparative Study*. 691–709. https://doi.org/10.1007/978-3-030-70542-8_28 (2021).
22. Idir, A., Canale, L., Tadjer, S. A. & Chekired, F. High order approximation of fractional PID controller based on grey wolf optimization for DC motor. In *2022 IEEE International Conference on Environment and Electrical Engineering and 2022 IEEE Industrial and Commercial Power Systems Europe (EEEIC/I&CPS Europe)*. 1–6. https://doi.org/10.1109/EEEIC/ICPSEurope54979.2022.9854520 (IEEE, 2022).
23. Saini, R., Parmar, G. & Gupta, R. An enhanced hybrid stochastic fractal search FOPID for speed control of DC motor. In *Fractional Order Systems and Applications in Engineering*. 51–67. https://doi.org/10.1016/B978-0-32-390953-2.00011-6 (Elsevier, 2023).
24. Eker, E., Kayri, M., Ekinci, S. & Izci, D. A new fusion of ASO with SA algorithm and its applications to MLP training and DC motor speed control. *Arab. J. Sci. Eng.* **46**, 3889–3911. https://doi.org/10.1007/s13369-020-05228-5 (2021).
25. Ekinci, S., Hekimoğlu, B. & Izci, D. Opposition based Henry gas solubility optimization as a novel algorithm for PID control of DC motor. *Eng. Sci. Technol. Int. J.* **24**, 331–342. https://doi.org/10.1016/j.jestch.2020.08.011 (2021).
26. Idir, A., Khettab, K. & Bensafia, Y. Design of an optimally tuned fractionalized PID controller for dc motor speed control via a henry gas solubility optimization algorithm. *Int. J. Intell. Eng. Syst.* **15**, 59–70. https://doi.org/10.22266/ijies2022.0630.06 (2022).
27. Ekinci, S., Izci, D. & Hekimoğlu, B. Optimal FOPID speed control of DC motor via opposition-based hybrid manta ray foraging optimization and simulated annealing algorithm. *Arab. J. Sci. Eng.* **46**, 1395–1409. https://doi.org/10.1007/s13369-020-05050-z (2021).
28. Izci, D. Design and application of an optimally tuned PID controller for DC motor speed regulation via a novel hybrid Lévy flight distribution and Nelder-Mead algorithm. *Trans. Inst. Meas. Control.* **43**, 3195–3211. https://doi.org/10.1177/01423312211019633 (2021).
29. Ekinci, S., Izci, D. & Yilmaz, M. Efficient speed control for DC motors using novel gazelle simplex optimizer. *IEEE Access.* **11**, 105830–105842. https://doi.org/10.1109/ACCESS.2023.3319596 (2023).

30. Idir, A., Akroum, H., Tadjer, S. A. & Canale, L. A comparative study of integer order PID, fractionalized order PID and fractional order PID controllers on a class of stable system. In *2023 IEEE International Conference on Environment and Electrical Engineering and 2023 IEEE Industrial and Commercial Power Systems Europe (EEEIC / I&CPS Europe)*, 1–6. https://doi.org/10.1109/EEEIC/ICPSEurope57605.2023.10194844 (IEEE, 2023) .
31. Idir, A., Canale, L., Bensafia, Y. & Khettab, K. Design and robust performance analysis of low-order approximation of fractional PID controller based on an IABC algorithm for an automatic voltage regulator system. *Energies* **15**, 8973. https://doi.org/10.3390/en15238973 (2022).
32. Ekinci, S., Izci, D. & Hekimoglu, B. PID speed control of DC motor using Harris hawks optimization algorithm. In *2020 International Conference on Electrical, Communication, and Computer Engineering (ICECCE)*, 1–6. https://doi.org/10.1109/ICECCE49384.2020.9179308 (IEEE, 2020).
33. Trojovský, P. & Dehghani, M. Pelican optimization algorithm: a novel nature-inspired algorithm for engineering applications. *Sensors.* **22**, 855. https://doi.org/10.3390/s22030855 (2022).
34. Sharma, S., Sharma, N. K., Bajaj, M., Kumar, V., Jurado, F. & Kamel, S. Optimal BLDC motor control using a WOA-based LQR strategy. In *IEEE Global Power, Energy and Communication Conference - GPECOM2022, Cappadocia, Turkey June 14–17*, 222–226, https://doi.org/10.1109/GPECOM55404.2022.9815609 (2022).
35. Davoudkhani, I. F. et al. Robust load-frequency control of islanded urban microgrid using 1PD-3DOF-PID controller including mobile EV energy storage. *Sci. Rep.* **14**, 13962. https://doi.org/10.1038/s41598-024-64794-y (2024).
36. Gopi, P. et al. Performance and robustness analysis of V-Tiger PID controller for automatic voltage regulator. *Sci. Rep.* **14**, 7867. https://doi.org/10.1038/s41598-024-58481-1 (2024).
37. Agarwal, J., Parmar, G., Gupta, R. & Sikander, A. Analysis of grey wolf optimizer based fractional order PID controller in speed control of DC motor. *Microsyst. Technol.* **24**, 4997–5006. https://doi.org/10.1007/s00542-018-3920-4 (2018).
38. Agarwal, J., Parmar, G. & Gupta, R. Application of sine cosine algorithm in optimal control of DC motor and robustness analysis. *Wulfenia J.* **24**, 77–95 (2017).
39. Bhatt, R., Parmar, G., Gupta, R. & Sikander, A. Application of stochastic fractal search in approximation and control of LTI systems. *Microsyst. Technol.* **25**, 105–114. https://doi.org/10.1007/s00542-018-3939-6 (2019).
40. Xiu, J., Wang, S. & Xiu, Y. Optimum firing angles control for switched reluctance motor based on IPSO at steady state. *IEEE Trans. Energy Convers.* **38**, 780–788. https://doi.org/10.1109/TEC.2023.3235790 (2023).
41. Scalcon, F. P., Vieira, R. P. & Gründling, H. A. PSO-based fast mechanical parameters estimation of switched reluctance motor drives. *J. Control Autom. Electr. Syst.* **33**, 1286–1293. https://doi.org/10.1007/s40313-022-00896-0 (2022).
42. Jabari, M. & Rad, A. Optimization of speed control and reduction of torque ripple in switched reluctance motors using metaheuristic algorithms based PID and FOPID controllers at the edge. *Tsinghua Sci. Technol.* https://doi.org/10.26599/TST.2024.9010021 (2024).
43. Tepljakov, A. FOMCON: fractional-order modeling and control toolbox. In *Fractional-order Modeling and Control of Dynamic Systems*, 107–129. https://doi.org/10.1007/978-3-319-52950-9_6(Springer, 2017).

Author contributions

Mostafa Jabari: Conceptualization, Methodology, Software, Visualization, Investigation, Writing- Original draft preparation. Serdar Ekinci, Davut Izci: Data curation, Validation, Supervision, Resources, Writing - Review & Editing. Mohit Bajaj, Ievgen Zaitsev: Project administration, Supervision, Resources, Writing - Review & Editing.

Declarations

Competing interests

The authors declare no competing interests.

Additional information

Correspondence and requests for materials should be addressed to M.B. or I.Z.

Reprints and permissions information is available at www.nature.com/reprints.

Publisher's note Springer Nature remains neutral with regard to jurisdictional claims in published maps and institutional affiliations.

Open Access This article is licensed under a Creative Commons Attribution-NonCommercial-NoDerivatives 4.0 International License, which permits any non-commercial use, sharing, distribution and reproduction in any medium or format, as long as you give appropriate credit to the original author(s) and the source, provide a link to the Creative Commons licence, and indicate if you modified the licensed material. You do not have permission under this licence to share adapted material derived from this article or parts of it. The images or other third party material in this article are included in the article's Creative Commons licence, unless indicated otherwise in a credit line to the material. If material is not included in the article's Creative Commons licence and your intended use is not permitted by statutory regulation or exceeds the permitted use, you will need to obtain permission directly from the copyright holder. To view a copy of this licence, visit http://creativecommons.org/licenses/by-nc-nd/4.0/.

© The Author(s) 2024